

Multiple change point detection in functional data with applications to biomechanical fatigue data

Patrick Bastian¹, Rupsa Basu², and Holger Dette¹

¹Ruhr-Universität Bochum, Germany

²University of Twente., The Netherlands and Universität zu Köln, Germany

April 25, 2024

Abstract

Injuries to the lower extremity joints are often debilitating, particularly for professional athletes. Understanding the onset of stressful conditions on these joints is therefore important in order to ensure prevention of injuries as well as individualised training for enhanced athletic performance. We study the biomechanical joint angles from the hip, knee and ankle for runners who are experiencing fatigue. The data is cyclic in nature and densely collected by body worn sensors, which makes it ideal to work with in the functional data analysis (FDA) framework.

We develop a new method for multiple change point detection for functional data, which improves the state of the art with respect to at least two novel aspects. First, the curves are compared with respect to their maximum absolute deviation, which leads to a better interpretation of local changes in the functional data compared to classical L^2 -approaches. Secondly, as slight aberrations are to be often expected in a human movement data, our method will not detect arbitrarily small changes but hunts for relevant changes, where maximum absolute deviation between the curves exceeds a specified threshold, say $\Delta > 0$. We recover multiple changes in a long functional time series of biomechanical knee angle data, which are larger than the desired threshold Δ , allowing us to identify changes purely due to fatigue. In this work, we analyse data from both controlled indoor as well as from an uncontrolled outdoor (marathon) setting.

Keywords and Phrases: Multiple change detection, relevant changes, functional data, biomechanical joint angles, human gait analysis

1 Introduction

In this paper we develop a novel methodology for detecting (multiple) change points in functional time series. Our work is motivated by data analysis in the field of human movement, a highly relevant subject area focused on comprehending the impact of disease and aging on physical ability as well as enhancing performance in sports. Human movement is often characterized by its continuous and repetitive motions, which in conjunction with dense data

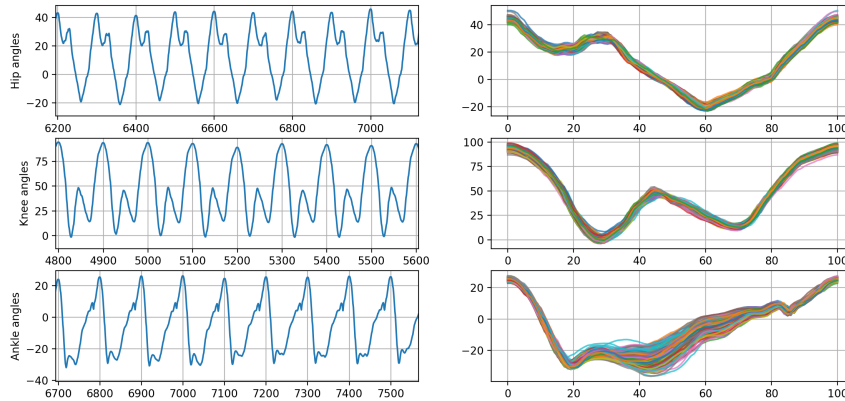


Figure 1: *Biomechanical angle data from the hip (top), knee (middle), ankle (bottom) for a single runner. Left panes: Consecutive strides of a runner from a part of the run. Right panels: Resulting functional time series of the different strides.*

collection via sensors naturally leads to a functional data framework. In Figure 1 we display typical data for the different lower extremity joints from one runner. The left part of the figure shows strides (cycles) corresponding to angular data measured at the hip, knee and ankles between consecutive contacts of the foot with the ground. The resulting functional time series of the different strides of the runner are shown in the right part of Figure 1. Within human movement analysis, it is particularly important to detect problematic movements under stress conditions like fatigue and to understand the adjustments made by the body in this case. In order to do that, it is essential to detect *when* fatigue has kicked-in and the onset of these stressors are characterised by deviations in this type of data. However, this problem is a difficult one, as such subtle changes, often characterised by spikes within the functions, are not very visible in plots of consecutive strides as displayed in Figure 1, respectively. Therefore, detecting changes in running data and inferring that when a change occurs, it is indeed due to fatigue is a very challenging task amounting to looking for subtle yet significant changes in a long functional time series.

Mathematically, this means that we are supremely concerned with locating multiple change points in a functional time series as it is to be expected that the adaptation of the body cannot be a one-time event. In this regard, it is of importance to note that very often there appear “small” deviations in movement data which are not caused by fatigue, but due to measurement errors and other environmental aspects during data collection. A typical example causing such small changes in the functional time series is the shifting of sensors due to sweating. Although, mathematically, the time points corresponding to these deviations could be considered as change points, they are not of practical interest because the deviations at these points are very small as compared to the adaptations made by the body under fatigue. More precisely, in the examples under consideration, changes caused by environmental aspects usually cause only minor deviations, while changes due to fatigue lead to larger deviations. Thus statistical methodology is required which is able to detect only the “scientifically relevant” change points, that is the locations corresponding to changes due to fatigue. We therefore look at deviations (or spikes) in the functional data that are larger than a certain threshold.

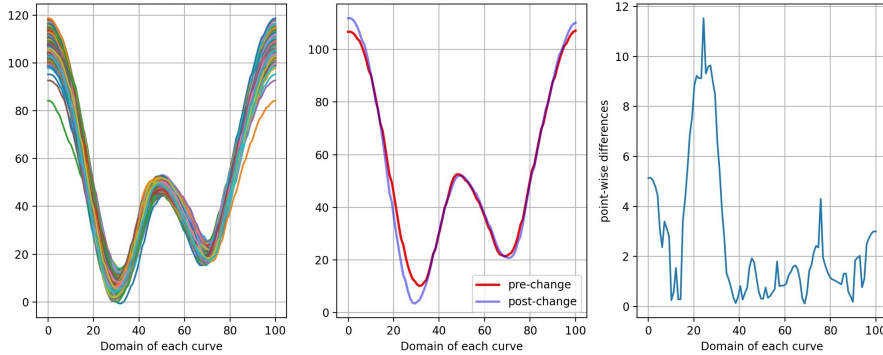


Figure 2: *Left: knee angle data from each cycle over the course of the run. Middle: mean curves, prior to- and after- the change point for a single runner. Right: absolute difference between the mean curves.*

This point of view raises the question how to measure deviations between two observations of the functional time series. Most of the literature has dealt with developing L^2 -space based methodology for which there exists by now a fully fledged theory. If one is interested in arbitrary small deviations the choice of the norm does not matter (because the norm of the difference between two curves vanishes if and only if the difference vanishes as well). However, if one is interested in differences with a norm exceeding a certain threshold, the choice of the norm is a more delicate problem. We argue that in the present context of human movement data it is more reasonable to measure deviations with respect to the maximum deviation of the curves because of the sensitivity of the sup-norm to local spikes. A typical situation is displayed in Figure 2. The middle panel shows the estimated mean of the curves of the functional time series (displayed in the left panel) before and after a relevant change point, which has been estimated by the procedure to be developed in this paper. In the right part we plot the absolute difference of the two mean curves, and we observe one rather large spike. Such local spikes are typical for this type of data and may be easier to detect using the sup-norm instead of the L^2 -norm. Therefore, by using the sup-norm, we capture local behaviour within the functional data, which may come in the form of short but significant spikes. This is particularly relevant for the biomechanical data under consideration given that human movement will not change dramatically at the stride level (in terms of shape, which would be captured well by L^2) but locally within the strides and may therefore only be detectable by using the sup-norm. In this case the change point problem becomes much more challenging as we are abandoning the Hilbert-space setting in favor of a Banach-space framework, for which the theory is not so well developed.

Our contribution In this paper we will develop a new approach for detecting multiple change points in functional time series that distinguishes itself from the currently available methodology in various aspects. First, since all functions considered in our applications are at least continuous and probably smoother than that, the new change point detector will be tailored to applications for functional data in the space of continuous functions $C([0, 1])$ where deviations are measured by the sup-norm. Second, compared to the literature, the procedure proposed in this paper detects relevant change points, which means deviations (measured by the sup-norm) exceeding a certain (positive) threshold. On the one hand this addresses the practical demands in the human movement data where one is only interested in changes caused by fatigue. On the other hand, looking only at relevant changes reflects

the fact that in many applications it is not plausible that two functions of a time series are exactly the same (even if we compare their expectations). This point of view is in line with Tukey (1991), who argued in the context of multiple comparisons of means that ... *“All we know about the world teaches us that the effects of A and B are always different - in some decimal place - for any A and B. Thus asking “Are the effects different?” is foolish”*. . . . Third, giving up on the theoretically convenient L^2 -space and entering the Banach-space setting means that substantially more effort is necessary to establish the validity of our approach including statistical guarantees. This applies even more when one also aims for detecting only the relevant change points as we leave methodologically convenient stationarity assumptions. Fourth, to our knowledge, this is the first time that fatigue detection for lower extremity joint angles is carried out using the framework of change point detection for functional data analysis. In particular, the above breakthroughs allow us to study this type of data in a far more coherent manner, permitting deductions on the characteristics, which may not have been possible based on other methods. Fourth, such an analysis using advanced statistical methodology is a first of its kind for studying fatigue detection in biomechanical lower extremity joint angle data. While experts in biomechanical sciences have known that fatigue brings about pronounced changes in the way we move, it was so far unclear how this change actually impacts the movements of the joints, in particular the knee joint. Such a methodology allows us to study the individualised characteristics of each runner under stressful, prolonged running conditions. The novel aspect of this methodology is the dual contribution of relevant changes of size Δ as well as that of working with fully functional methodology in the supnorm. The former, allows us to pick up changes which are larger than a certain size Δ while the latter enables us to identify the exact part of a cyclic movement that is changing under fatigue. This contributes majorly to our understanding how our body copes with fatigue as well as the straining effects of enduring such a coping mechanisms ultimately resulting in muscle wear and tear as well as injuries.

Related literature Change point analysis of time series data is by now a well studied field with an enormous amount of publications by numerous authors. Meanwhile, the literature on addressing the problem of detecting multiple structural breaks is also extensive and exemplary we mention (wild) binary segmentation (Fryzlewicz, 2014), pruned exact linear time tests (Killick et al., 2012; Maidstone et al., 2017), moving sum scan (Eichinger and Kirch, 2018) and simultaneous multiscale change point estimators (Frick et al., 2014; Li et al., 2017; Dette et al., 2020a), narrowest over threshold (Baranowski et al., 2019) and the references in these works. The optimality of univariate multiple change point detection procedures has recently been investigated by Wang et al. (2020). Extensions have been made on multiple change detection for multivariate and high dimensional data; see Cho and Fryzlewicz (2014); Cho (2016); Wang and Samworth (2017); Padilla et al. (2021); Kovács et al. (2023) among many others.

For functional data, change point analysis has mainly been carried out under the assumption of one change point (see, for example, Aue et al., 2009; Berkes et al., 2009; Aston and Kirch, 2012; Horváth et al., 2014; Shapurov et al., 2016; Bucchia and Wendler, 2017; Aue et al., 2018; Stoehr et al., 2021). Methodology for detecting one relevant change point has been developed by Dette et al. (2020b,c) and (Dette and Kutta, 2021) among others. Most of these work refers to L^2 -space methodology (see Dette et al., 2020b, for an exception).

The literature on detecting multiple change points in functional time series is more scarce and - to our best knowledge - we are only aware of the work Chiou et al. (2019); Harris et al. (2022); Rice and Zhang (2022) and Madrid Padilla et al. (2022). The first three

references are mostly concerned with segmentation methods for densely observed data while Madrid Padilla et al. (2022) also consider sparsely observed functional data, in particular none of them consider relevant change points nor do they measure the deviation between the curves by the sup-norm as we do.

2 Relevant change points in functional data

Let $C(T)$ denote the space of continuous functions defined on the set T . Throughout this paper T is either the interval $T = [0, 1]$ or a rectangular of the form $T = [u, v] \times [0, 1]$ with $0 \leq u < v \leq 1$. We define by $\|\cdot\|_\infty$ the sup-norm on $C(T)$ (the corresponding space will always be clear from the context), and denote for $f \in C([u, v] \times [0, 1])$ by

$$\|f(s, \cdot)\|_\infty = \max_{t \in [0, 1]} |f(s, t)|$$

the sup-norm of the function $t \rightarrow f(s, t)$ (for fixed s). We consider a triangular-array $\{X_{n,j} | j = 1, \dots, n\}_{n \in \mathbb{N}}$ of $C([0, 1])$ -valued random variables with the representation

$$X_{n,j} = \mu_{n,j} + \epsilon_{n,j}, \quad j = 1, \dots, n, \quad (2.1)$$

where $\{\epsilon_{n,j}\}_{j=1, \dots, n}$ is a row-wise centred stationary process and $\mu_{n,j} = \mathbb{E}[X_{n,j}] \in C([0, 1])$ denotes the mean function of $X_{n,j}$. For the sake of a simple notation, we will suppress in this section the dependence of the functions on the sample size $n \in \mathbb{N}$ and use the notations X_j, ϵ_j instead of $X_{n,j}, \epsilon_{n,j}$. Further, assumptions regarding the probabilistic structure of the random elements will be stated below in Section 4, where we discuss the theoretical properties of the proposed procedure.

We assume that there exists a set

$$S = \{s_1, s_2, \dots, s_m\} \subset (0, 1)$$

of change points in the sequence of mean functions with $s_1 \leq s_2 \leq \dots \leq s_m$, where m is finite in the sense that it does not depend on n . More precisely, for any $1 \leq i \leq m < \infty$ we assume

$$\mu_i := \mu_{\lfloor ns_{i-1} \rfloor + 1} = \mu_{\lfloor ns_{i-1} \rfloor + 2} = \dots = \mu_{\lfloor ns_i \rfloor} \neq \mu_{i+1}$$

where we adopt the convention $s_0 = 0$ and $s_{m+1} = 1$. For example, μ_1 is the mean function before the first change point $\lfloor ns_1 \rfloor$, μ_2 is the mean function between the change point $\lfloor ns_1 \rfloor$ and second change point $\lfloor ns_2 \rfloor$ and so on. We are interested in those change points in S , where the maximal absolute deviation between the mean functions before and after the change point exceeds a given threshold, say $\Delta > 0$. The choice of this threshold is problem specific as it defines, when a change is considered as relevant. For the human movement data used in this work we discuss this choice in more detail in Section 4.

Our goal is to detect all locations of relevant changes, that is to estimate the set

$$S_{\text{rel}} = \{s_i \in \{s_1, \dots, s_m\} | \|\mu_{i+1} - \mu_i\|_\infty > \Delta\}$$

and control the statistical error of the estimator. For this purpose we proceed in two steps: **Step 1:** We estimate (consistently) the number of all change points and their locations

by a particular binary segmentation algorithm. Note that in this step, we recover change points which may or may not be of a relevant size. We denote the estimated number and the estimated set of change points by \hat{m} and

$$\hat{S} = \{\hat{s}_1, \hat{s}_2, \dots, \hat{s}_{\hat{m}}\},$$

respectively (we define $\hat{s}_0 = 0$ and $\hat{s}_{\hat{m}+1} = 1$). This part of the procedure is described in Algorithm 1 below.

Step 2: We investigate for each interval $[\hat{s}_{i-1}, \hat{s}_{i+1}]$ ($i = 1, \dots, \hat{m}$) if it contains a relevant change point. This is done by defining for each interval detectors, say $\hat{T}_{n,1}, \dots, \hat{T}_{n,\hat{m}}$, which are then aggregated by the maximum operator, that is $\hat{T}_n = \max_{i=1, \dots, \hat{m}} \hat{T}_{n,i}$. Next we calculate a quantile, say $q_{1-\alpha}^*$ by a non-standard bootstrap procedure such that

$$\limsup_{n \rightarrow \infty} \mathbb{P}(\hat{T}_n > q_{1-\alpha}^*) \leq \alpha$$

whenever $S_{\text{rel}} = \emptyset$. Finally, we define the set of estimated relevant change points by

$$\hat{S}_{\text{rel}} = \{\hat{s}_i \in \{\hat{s}_1, \dots, \hat{s}_{\hat{m}}\} \mid \hat{T}_{n,i} > q_{1-\alpha}^*\}. \quad (2.2)$$

Note that in the case where Step 1 does not recover any change points, Step 2 is not executed. The details of Step 1 and 2 are explained in the following Section 2.1. and 2.2, respectively.

2.1 A first segmentation of the functional time series

Binary segmentation is a very well known algorithm for the multiple change detection scenario. This algorithm scans through the whole data set and looks for a first change point. When such a change point is detected, the data is divided into two samples before and after this initial change point and the procedure is repeated for each of the segments. The algorithm stops as soon as all the segments so far return a lack of change point. Since its introduction by Vostrikova (1981) binary segmentation has been used and investigated by numerous authors (see Fryzlewicz, 2014; Baranowski et al., 2019; Kovács et al., 2023, among many others). However the theoretical properties of the algorithm for functional data are less well understood. In order to identify all change points s_1, \dots, s_m and the number of change points m in the present context we define for $l, r \in \{1, \dots, n\}$ ($l < r$), $t \in [0, 1]$, the sequential processes (in $s \in [\frac{l+1}{n}, \frac{r}{n}]$)

$$\hat{U}_{l,r}(s, t) = \frac{1}{r-l} \left(\sum_{j=l+1}^{\lfloor sn \rfloor} X_j(t) + (r-l) \left(s - \frac{\lfloor s(r-l) \rfloor}{(r-l)} \right) X_r(t) - \frac{\lfloor sn \rfloor - l}{r-l} \sum_{j=l+1}^r X_j(t) \right), \quad (2.3)$$

and determine the change points by Algorithm 1. We will establish in Theorem 4.1 in Section 4 the validity of this procedure. In other words: Algorithm 1 provides consistent estimators for both the location and the number of the change points.

In the upper part of Figure 3 we illustrate the application of Algorithm 1 for a full functional time series of biomechanical knee angle data, collected from one athlete. The individual component curves which correspond to each cycle during the course of the run (seen clearly in the right panel of Figure 1) are not visible here as the data is collected via a fatiguing protocol and hence consists of a large number of cycles. The red vertical lines show the

Algorithm 1 Function: BINSEG(t_0, T, ξ_n), for estimating change points in the sequence X_{t_0}, \dots, X_T .

```

1: Fix  $t_0 \leftarrow$  first time point and  $T \leftarrow$  last time point of sample
2: Fix  $\hat{m} \leftarrow 0$  (estimate of the number of change points)
3: Fix  $\hat{S} \leftarrow \emptyset$  (set of estimated change points)
4: if  $T - t_0 \leq 1$  then
5:   STOP
6: else  $\hat{k} = \arg \max_{s \in t_0, \dots, T} \|U_{t,T}(s/n, \cdot)\|_2$ 
7:    $\mathcal{U} = \|U_{t_0, T}(\hat{k}/n, \cdot)\|_2$ 
8:   if  $\mathcal{U} > \xi_n$  then
9:      $\hat{m} \leftarrow \hat{m} + 1$ 
10:     $\hat{S} \leftarrow \hat{S} \cup \{\hat{k}\}$ 
11:    run BINSEG ( $t_0, \hat{k}, \xi_n$ ) and BINSEG ( $\hat{k}, T, \xi_n$ )
12:   end if
13: end if
14: Order the detected change points, i.e.  $\hat{S} = \{\hat{k}_1, \hat{k}_2, \dots, \hat{k}_{\hat{m}}\}$  with  $\hat{k}_1 < \hat{k}_2 < \dots < \hat{k}_{\hat{m}}$ 
15: For  $i = 1, \dots, \hat{m}$  define:  $\hat{s}_0 \leftarrow 0$ ;  $\hat{s}_i \leftarrow \hat{k}_i/n$ ;  $\hat{s}_{\hat{m}+1} \leftarrow 1$ 

```

estimated change points found using Algorithm 1. Note that as seen, not all change points determined in this step might be relevant. In the lower part of Figure 3 we display the differences of the estimates of the mean functions on the four segments identified by the three estimated change points. We observe that the differences between the two segments separated by the first change point are much larger than the other two. As will be seen later, some changes detected in this step could be due to unforeseen obstructions in data collection such as shifting of sensors due to sweating, pedestrians on the path etc.

2.2 Hunting for relevant change points

In this section we describe the details for Step 2 of our approach. In particular we will motivate a new bootstrap procedure, which is used to define quantiles, such that all relevant change points in the functional time series are detected with a statistical guarantee. More specifically, recall that $\hat{k}_1 < \hat{k}_2 < \dots < \hat{k}_{\hat{m}}$ denote the estimated change points from Algorithm 1 and that $0 = \hat{s}_0 < \hat{s}_1 < \dots < \hat{s}_{\hat{m}} < \hat{s}_{\hat{m}+1} = 1$ denote the corresponding values scaled to the interval $[0, 1]$. Further, for $i = 1, \dots, \hat{m}$ let \hat{h}_i denote the linear transformation from the interval $[\hat{s}_{i-1}, \hat{s}_{i+1}]$ onto $[0, 1]$, that is

$$\hat{h}_i(s) = \frac{s - \hat{s}_{i-1}}{\hat{s}_{i+1} - \hat{s}_{i-1}}.$$

and let

$$h_i(s) = \frac{s - s_{i-1}}{s_{i+1} - s_{i-1}}$$

be the deterministic analog ($i = 1, \dots, m$). We recall the definition of the CUSUM statistic (2.3) for a given functional data stream and note that it can be shown that

$$\mathbb{E}[\hat{U}_{\hat{k}_{i-1}, \hat{k}_{i+1}}(s, t)] \simeq (h_i(s \wedge s_i) - h(s)h_i(s_i))(\mu_i(t) - \mu_{i+1}(t)) + o_{\mathbb{P}}(1),$$

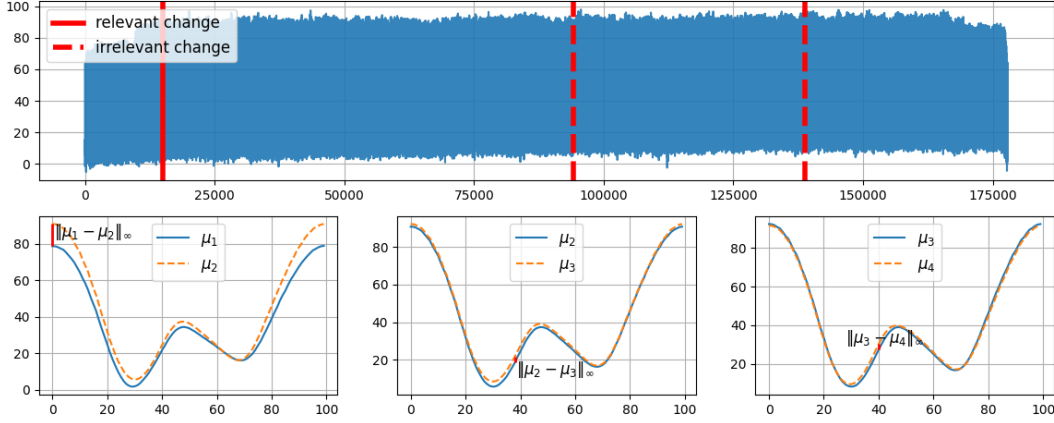


Figure 3: *Biomechanical knee angle data for a single runner. Upper part: The full functional time series with vertical lines denoting change points detected by Algorithm 1. The crosses denote the relevant change points detected by Algorithm 2: only the first change point is relevant. Lower part: Mean functions on the different segments determined by the estimated change points, with the red vertical lines showing the maximum deviation between them. The sample size for this runner is $n = 1800$.*

Therefore, the statistic

$$\hat{M}_{n,i} = \left\| \hat{U}_{\hat{k}_{i-1}, \hat{k}_{i+1}} \right\|_{\infty}$$

is a reasonable estimate of the size of the change $h_i(s_i)(1 - h_i(s_i))\|\mu_{i+1} - \mu_i\|_{\infty}$ at the point s_i . To check if the change in the i th interval is relevant we will compare $\hat{M}_{n,i}$ with $h_i(s_i)(1 - h_i(s_i))\Delta$ using the detector

$$\hat{T}_{n,i} = \sqrt{\hat{n}_i}(\hat{M}_{n,i} - \hat{h}_i(\hat{s}_i)(1 - \hat{h}_i(\hat{s}_i))\Delta) \quad (2.4)$$

where $\hat{n}_i = \lfloor n\hat{s}_{i+1} \rfloor - \lfloor n\hat{s}_{i-1} \rfloor$ (the scaling factor $\sqrt{\hat{n}_i}$ becomes clear later, see Remark 2.1 below). The different statistics are then aggregated by the maximum operator, that is

$$\hat{T}_n := \max_{1 \leq i \leq \hat{m}} \hat{T}_{n,i} . \quad (2.5)$$

We would like to use quantiles of this statistic to detect relevant change points. However, it turns out that even asymptotically the distribution of \hat{T}_n depends in a complicated manner on several parameters, which are difficult to estimate (see Remark 2.1 below). As an alternative we will develop a non-standard bootstrap method to obtain (asymptotically) upper bounds for these quantiles. To explain our approach we denote the sample means before and after the estimated change point \hat{k}_i , calculated from the sample $\{X_{\hat{k}_{i-1}+1}, X_{\hat{k}_{i-1}+2}, \dots, X_{\hat{k}_{i+1}}\}$, by

$$\hat{\mu}_{1, \hat{k}_i} = \frac{1}{\hat{k}_i - \hat{k}_{i-1}} \sum_{j=\hat{k}_{i-1}+1}^{\hat{k}_i} X_j \quad \text{and} \quad \hat{\mu}_{2, \hat{k}_i} = \frac{1}{\hat{k}_{i+1} - \hat{k}_i} \sum_{j=\hat{k}_i+1}^{\hat{k}_{i+1}} X_j .$$

Further, let $(\xi_k^{(1)} : k \in \mathbb{N}), \dots, (\xi_k^{(R)} : k \in \mathbb{N})$ denote independent sequences of i.i.d. standard normal distributed random variables. On the rectangle $[\hat{s}_{i-1}, \hat{s}_{i+1}] \times [0, 1]$ we consider the

processes $\hat{B}_{i,n}^{(1)}, \dots, \hat{B}_{i,n}^{(R)}$ defined by

$$\begin{aligned} \hat{B}_{i,n}^{(r)}(s, t) &= \frac{1}{\sqrt{\hat{n}_i}} \sum_{k=\hat{k}_{i-1}}^{\lfloor sn \rfloor} \frac{1}{\sqrt{L}} \left(\sum_{j=k}^{k+L-1} \hat{Y}_j - \frac{L}{\hat{n}_i} \sum_{j=\hat{k}_{i-1}}^{\hat{k}_{i+1}} \hat{Y}_j(t) \right) \xi_k^{(r)} \\ &+ \sqrt{\hat{n}_i} \left(s - \frac{\lfloor s \hat{n}_i \rfloor}{\hat{n}_i} \right) \frac{1}{\sqrt{L}} \left(\sum_{j=\lfloor sn \rfloor + 1}^{\lfloor sn \rfloor + L} \hat{Y}_j - \frac{L}{n} \sum_{j=\hat{k}_{i-1}}^{\hat{k}_{i+1}} \hat{Y}_j(t) \right) \xi_{\lfloor sn \rfloor + 1}^{(r)}, \end{aligned}$$

where

$$\hat{Y}_j = X_j - (\hat{\mu}_{2, \hat{k}_i} - \hat{\mu}_{1, \hat{k}_i}) \mathbf{1}_{\{j > \lfloor \hat{s}_i n \rfloor\}}, \quad j = 1, \dots, n;$$

and $L \in \mathbb{N}$ defines the length of the blocks and satisfies $L/n \rightarrow 0$ and $L \rightarrow \infty$ as $n \rightarrow \infty$. We then consider a centered bootstrap analogue

$$\widehat{W}_{i,n}^{(r)}(s, t) = \hat{B}_{i,n}^{(r)}(s, t) - \hat{h}_i(s) \hat{B}_{i,n}^{(r)}(\hat{s}_{i+1}, t),$$

of the process $\hat{U}_{\hat{k}_{i-1}, \hat{k}_{i+1}}$ and define for each estimated change point \hat{s}_i the set

$$\hat{\mathcal{E}}_i^\pm = \left\{ t \in [0, 1] : \pm(\hat{\mu}_{1, \hat{k}_i}(t) - \hat{\mu}_{2, \hat{k}_i}(t)) \geq \|\hat{\mu}_{1, \hat{k}_i} - \hat{\mu}_{2, \hat{k}_i}\|_\infty - \frac{c \log n}{\sqrt{n}} \right\}, \quad (2.6)$$

where $c > 0$ denotes a constant. It can be shown that these sets are consistent estimates of the extremal sets

$$\mathcal{E}_i^\pm := \left\{ t \in [0, 1] \mid \mu_i(t) - \mu_{i+1}(t) = \pm \|\mu_i - \mu_{i+1}\|_\infty \right\},$$

which contain the points, where the function $t \rightarrow (\mu_{i+1}(t) - \mu_i(t))$ attains its sup-norm $\|\mu_{i+1} - \mu_i\|_\infty$. Note that these sets depend on the (unknown) mean functions before and after the i th change point. We then suggest to consider the bootstrap statistics

$$\hat{T}_i^{(r)} = \max \left\{ \sup_{t \in \hat{\mathcal{E}}_i^+} \widehat{W}_{i,n}^{(r)}(\hat{s}_i, t), \sup_{t \in \hat{\mathcal{E}}_i^-} (-\widehat{W}_{i,n}^{(r)}(\hat{s}_i, t)) \right\} \quad (2.7)$$

$$\hat{T}_n^{*,(r)} = \max_{i=1}^{\hat{m}} \hat{T}_i^{(r)} \quad (2.8)$$

and define $q_{1-\alpha}^*$ as the $(1-\alpha)$ -quantile of bootstrap statistic $\hat{T}_n^{*,(r)}$. Finally, the set of relevant change points is estimated by (2.2). The implementation of this procedure is described in Algorithm 2, which defines an estimate of $q_{1-\alpha}^*$ by resampling.

Remark 2.1. We give some motivation why this bootstrap procedure can be used to generate quantiles in the present context. If all changes are not relevant, that is $\max_{1 \leq k \leq m} \|\mu_k - \mu_{k-1}\|_\infty \leq \Delta$, it can be shown (see Section 5 for details) that the statistic \hat{T}_n in (2.5) is bounded by $\hat{D}_n := \max_{1 \leq i \leq \hat{m}} \hat{D}_{n,i}$ with probability converging to 1 as $n \rightarrow \infty$, where

$$\hat{D}_{n,i} := \sqrt{\hat{n}_i} \left(\hat{M}_{n,i} - \hat{h}_i(\hat{s}_i)(1 - \hat{h}_i(\hat{s}_i)) \|\mu_{i+1} - \mu_i\|_\infty \right). \quad (2.9)$$

Algorithm 2 Estimation of relevant change points

- 1: **Compute** the number \hat{m} and all (ordered) change points $\hat{S} = \{\hat{s}_1, \dots, \hat{s}_{\hat{m}}\}$ using BINSEG($1, n, \xi_n$)
 - 2: **Fix** block length L , number of bootstrap replications R and constant $c > 0$
 - 3: **for** $1 = 1, \dots, \hat{m}$ **do**
 - 4: **Compute** the estimates $\hat{\mathcal{E}}_i^\pm$ of the extremal sets defined in (2.6)
 - 5: **end for**
 - 6: **for** $r = 1, \dots, R$ **do**
 - 7: **Compute** $\widehat{W}_{i,n}^{(r)}(s, t)$
 - 8: **if** $\hat{\mathcal{E}}_i^\pm \neq \emptyset$ **then**
 - 9: $\hat{T}_{i,n}^{(r)} = \max\{\sup_{t \in \hat{\mathcal{E}}_i^+} \widehat{W}_{i,n}^{(r)}(\hat{s}_i, t), \sup_{t \in \hat{\mathcal{E}}_i^-} -\widehat{W}_{i,n}^{(r)}(\hat{s}_i, t)\}$
 - 10: **else set** $\hat{T}_{i,n}^{(r)} = \pm\infty$
 - 11: **end if**
 - 12: **Compute** $\hat{T}_n^{*,(r)} = \max_i \hat{T}_{i,n}^{(r)}$
 - 13: **end for**
 - 14: **Compute** $q_{1-\alpha}^* \leftarrow$ as the empirical $(1-\alpha)$ -quantile of bootstrap sample $\hat{T}_n^{*,(1)}, \dots, \hat{T}_n^{*,(R)}$
 - 15: **Estimate** the relevant change points by (2.2)
-

Moreover, there even is equality if $\|\mu_{i+1} - \mu_i\|_\infty = \Delta$ for all $i = 1, \dots, m$. One can show (see Section 5 for details) that

$$\begin{aligned}
 \hat{D}_{n,i} &\xrightarrow{\mathcal{D}} D(\mathcal{E}_i) := \max \left\{ \sup_{t \in \mathcal{E}_i^+} \mathbb{W}(h_i(s_i), t), \sup_{t \in \mathcal{E}_i^-} \mathbb{W}(h_i(s_i), t) \right\}, \\
 \hat{D}_n &:= \max_{i=1}^m \hat{D}_{n,i} \xrightarrow{\mathcal{D}} D(\mathcal{E}) := \max_{i=1}^m D(\mathcal{E}_i) \\
 &= \max_{i=1}^m \max \left\{ \sup_{t \in \mathcal{E}_i^+} \mathbb{W}(h_i(s_i), t), \sup_{t \in \mathcal{E}_i^-} \mathbb{W}(h_i(s_i), t) \right\}.
 \end{aligned} \tag{2.10}$$

Here the symbol $\xrightarrow{\mathcal{D}}$ denotes weak convergence of real valued random variables and \mathbb{W} is a mean zero Gaussian process on $[0, 1] \times [0, 1]$ with covariance structure given by

$$\text{Cov}(\mathbb{W}(s, t), \mathbb{W}(s', t')) = (s \wedge s' - ss') \sum_{i=-\infty}^{\infty} \text{Cov}(\epsilon_0(t), \epsilon_i(t')).$$

The bootstrap statistics $\hat{T}_i^{(r)}$ and $\hat{T}_n^{*,(r)}$ in 2.7, 2.8 mimic asymptotically the distributional properties of the random variables $\hat{D}_{n,i}$ and \hat{D}_n defined in (2.9) and (2.10), respectively. As \hat{T}_n is asymptotically bounded by \hat{D}_n , we have

$$\mathbb{P}(\hat{T}_n \leq q_{1-\alpha}^*) \geq \mathbb{P}(\hat{D}_n > q_{1-\alpha}^*) + o(1) = 1 - \alpha + o(1)$$

as $n \rightarrow \infty$, and this statement is sufficient for proving consistency of the estimated set of relevant change points (2.2) for S_{rel} . Details can be found in Section 4.

Remark 2.2.

- (a) It is possible to develop a similar algorithm for the L^2 - instead of the sup-norm. In fact, such a procedure would not require the estimation of the extremal sets. However, the choice of the threshold for this norm is conceptually (not mathematically) more difficult, and we emphasize that one of the main motivations for using the sup-norm in our approach is the easy and very natural interpretation of the threshold in the considered application.
- (b) In this paper we assume that at each time point the full trajectory is observed. Our method is also applicable (and its validity can be established) to dense and discrete observations from the trajectory. In particular, in the considered application the hip, knee and ankle angles are continuously recorded resulting in an extremely dense grid, where the trajectories are observed.
- (c) Note that alternatively to the above retrospective change detection, sequential change point analysis of such a data is of prominent interest in the goal of injury prevention. One aim in this collaboration project *Sports, Data, and Interaction*¹ is to set up an interactive system to provide real-time feedback to the athlete. In this scenario, the idea is to have the least invasive approach of recording biomechanical joint angles, for example, via a video camera. When such a data is studied by sequential analysis, the athlete or trainer could be alerted of a change and that the joint under consideration is moving differently and appropriate updates to training strategies may be made. This is however a future direction that may be pursued and we do not look at this scenario here.
- (d) The data set under consideration consists of 3-dimensional functional time series (for the hip, knee and ankle angles). In the discussion so far we have developed methodology for finding multiple change points in each component separately. Our approach can be generalized to find multiple change points in multivariate functional time series, and we briefly indicate here how this can be done.

For the first step we propose to use binary segmentation for each of the coordinates (of course, any other consistent procedure can be used). For the second step we have multiple ways to define what a relevant change is, depending on whether or not we would like to consider changes in the different coordinates jointly or separately. For the latter one could simply search for relevant changes (in the sense we have used previously) in any of the coordinates, i.e. for each coordinate $\ell = 1, 2, 3$ we define the analog of the statistic (2.4), say

$$\hat{T}_{n,i}^{(\ell)} = \sqrt{\hat{n}_i} (\hat{M}_{n,i}^{(\ell)} - \hat{h}_i(\hat{s}_i)(1 - \hat{h}_i(\hat{s}_i))\Delta_\ell)$$

with thresholds $\Delta_1, \Delta_2, \Delta_3$, respectively, and then additionally take the maximum over all three coordinates in (2.5), that is

$$\hat{T}_n := \max_{1 \leq i \leq \hat{m}} \max_{\ell=1}^3 \hat{T}_{n,i}^{(\ell)}. \quad (2.11)$$

If we want to consider the changes in all coordinates simultaneously we could first aggregate the statistics $\hat{M}_{n,i}^{(\ell)}$ using a functional such as $\phi(x) = \|x\|_q = (\sum_{\ell=1}^3 |x_\ell|^q)^{1/q}$

¹<http://www.sports-data-interaction.com/>

($1 \leq q \leq \infty$) and then rescale it, that is

$$\hat{T}_{n,i} = \sqrt{\hat{n}_i} \{ \phi((\hat{M}_{n,i}^{(1)}, \hat{M}_{n,i}^{(2)}, \hat{M}_{n,i}^{(3)})) - \hat{h}_i(\hat{s}_i)(1 - \hat{h}_i(\hat{s}_i))\Delta \}.$$

After this we can proceed as in (2.5). Multivariate analogs of Algorithm 2 can be developed for both cases and their validity can be shown by similar arguments as given in the proof Theorem 4.2. As the foremost goal of the *Sports, Data and Interaction* team was injury prevention in the knee joint we do not pursue these approaches here further.

3 Finite sample properties

In this section we study the finite sample properties of Algorithm 2 by means of a simulation study and illustrate its practical application in two data examples consisting of fatigue data from a laboratory setup as well as from a marathon run.

Note that Algorithm 1 and 2 require the specification of several tuning parameters. This includes firstly, the threshold value for locating change points in the binary segmentation ξ_n in Algorithm 1. Following a recommendation in Rice and Zhang (2022) we use $\xi_n = \hat{\sigma}_n \sqrt{3 \log(n)}$, where $\hat{\sigma}_n^2 = \text{median}(\|X_{i+1} - X_i\|_2^2/2, i = 2, \dots, n)$. For the parameter c required in the estimation of the extremal sets in (2.6) we choose $c = 0.1$ as recommended by Dette et al. (2020b). Furthermore, an initial robustness analysis showed that the procedure is rather stable with respect to this choice of c (the details are omitted for the sake of brevity). The number of bootstrap repetitions is always fixed as $R = 1000$. The block-length parameter L in the multiplier bootstrap is selected by a method proposed by Rice and Shang (2017), which requires the choice of a weight function. We have implemented their algorithm for the Bartlett, Parzen, Tukey-Hanning and Quadratic spectral kernel and observed that the quadratic spectral weight function yields the most stable results (these findings are not displayed for the sake of brevity). Finally, unless stated otherwise we use $\alpha = 10\%$ for the quantile $q_{1-\alpha}^*$.

3.1 Simulation study

For the simulation study we generate data according to the model in (2.1) with two and three change points. In the example with two change locations, we choose $s_1 = \lfloor \frac{n}{3} \rfloor$, $s_2 = \lfloor \frac{2n}{3} \rfloor$ and the mean functions are given by

$$\mu_j(t) = \begin{cases} 20(\sin(2\pi t) + \cos(2\pi t)) \\ 20(\sin(2\pi t) + \cos(2\pi t)) + \Delta_J(t)\mathbb{1}_{[0,0.16]}(t) \\ 20(\sin(2\pi t) + \cos(2\pi t)) + 2\Delta_J(t)\mathbb{1}_{[0,0.16]}(t) \end{cases} \quad j = 1, 2, 3, \quad (4.1)$$

where $\Delta_J\mathbb{1}_{[0,0.16]}$ is a symmetric cubic spline on the interval $[0, 0.16]$ interpolating the points $(0.01, 2)$, $(0.02, 5)$, $(0.03, 9)$, $(0.04, 10)$, $(0.05, 12)$, $(0.06, 15)$, $(0.07, 22)$, $(0.08, 25)$ and their reflections with respect to the vertical line through the point 0.085. In the example with three change points we choose $s_1 = \lfloor \frac{n}{4} \rfloor$, $s_2 = \lfloor \frac{2n}{4} \rfloor$ and $s_3 = \lfloor \frac{3n}{4} \rfloor$ and the mean functions μ_1, μ_2, μ_3 are given by (4.1), while $\mu_4(t) = 20(\sin(2\pi t) + \cos(2\pi t)) + \Delta_J(t)\mathbb{1}_{[0,0.16]}(t)$.

In both examples $(\epsilon_j)_{j \geq 1}$ is an fMA(1) process defined in the simulation section of (Dette et al., 2020b). To be precise, for the B-spline basis functions ν_1, \dots, ν_{21} we consider the linear

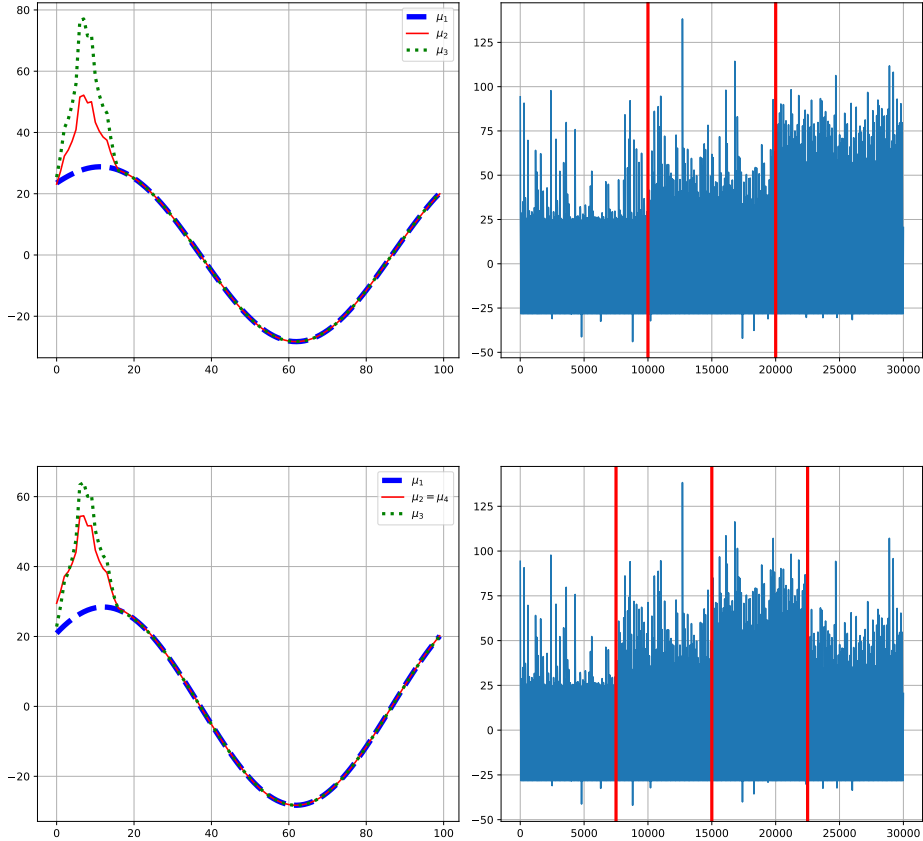


Figure 4: *Simulated data for $n = 300$ observations with two changes (first row) and three changes (second row). Left panels: mean curves on the different segments. Right panels: Full time series data with change points given by vertical lines.*

space $H = \text{span}\{\nu_1, \dots, \nu_{21}\} \subset C([0, 1])$ and define independent processes $\eta_1, \dots, \eta_n \in H$ by

$$\eta_j = \sum_{i=1}^{21} \mathbf{1}_{[-4,4]}(N_{i,j}) \nu_i, \quad j = 1, \dots, n,$$

where $N_{1,j}, \dots, N_{21,j}$ are independent, normally distributed random variables with $\mathbb{E}[N_{i,j}] = 0$ and $\text{Var}(N_{i,j}) = \frac{1}{i^2}$ ($i = 1, \dots, 21; j = 1, \dots, n$). The fMA(1) process is finally given by $\epsilon_i = \eta_i + \Theta \eta_{i-1}$, where the operator $\Theta : H \rightarrow H$ (acting on a finite-dimensional space) is defined by $0.8 \Psi / \sigma_1(\Psi)$, the elements in the position (i, j) of the matrix Ψ are normally distributed random variables with mean zero and standard deviation $1/(ij)$ and $\sigma_1(\Psi)$ denotes the spectral norm of Ψ .

The simulated data is displayed in Figure 4, where we also show the mean curves on the different segments. The results of the simulations (with sample sizes $n = 200, 300, 600$) are displayed in Figure 5 (two changes in the upper part, three changes in the lower part), which contains histograms of the estimated relevant change points obtained from 1000 repetitions. As is evident from the clustering of the histograms, we recover the true location of the change points fairly accurately and as predicted by the asymptotic theory in Section 4, performance improves with increasing sample size.

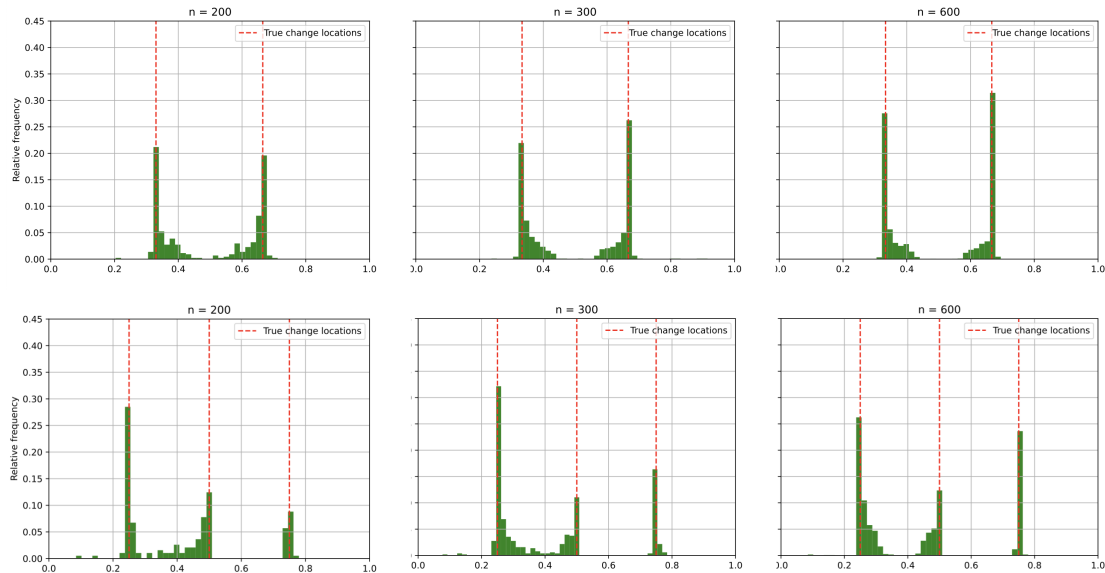


Figure 5: *Histograms of estimated relevant change points from 1000 simulation with relative frequencies with respect to all changes recovered in Step 1. Upper part: Two relevant changes. Lower part: Three relevant changes.*

3.2 Data examples

In this section, we investigate two data examples where the methodology developed in this paper is directly applied for statistical inference. One example refers to data collected in the laboratory, the other to data collected during a marathon run. Note that, hereafter the domain of each curve is the normalized time within each cycle of the data. A cycle in this regard means two subsequent contacts of the same foot with the ground.

3.2.1 Sensor data

We investigate biomechanical lower joint angle data from the knees from a running athlete, which was collected within the multidisciplinary project *Sports, Data, and Interaction*² with the goal of detecting persistent changes in the movement of the runner due to fatigue. Fatigue detection in running athletes is important for the elimination of problematic movements and reducing the risk of injuries. Similar analysis of the hip and ankle angle data is possible, even though this is not pursued further in this work.

The study subjects were recruited from a pool of frequent hobby runners between the ages of 21-60 years with experience ranging between 1- 14 years and subjects reported running between 2-5 times per week. In this section, we do not consider professional runners. This is because we expect pronounced changes post-fatigue in the hobby runners while professional runners, being especially trained are able to endure higher fatigue levels and time constraints do not allow for recording such long datasets in the laboratory.

The data was collected by body-worn sensors via inertial measurement units (IMUs) produced by Xsens (Xsens MVN link sensors, sampling at 240 Hz, see Schepers et al., 2018) while following a fatigue protocol, i.e. ensuring that an athlete was surely and steadily tired

²<http://www.sports-data-interaction.com/>

while minimising the impact of external factors on the data collection. The controlled laboratory setting minimizes the inevitable disturbances occurring during other data collection procedures like outdoors on a running track. Further, the treadmill controlled the speed of the runner and hence any deviations due to external factors other than fatigue were kept to a minimum. Unless otherwise stated, in the following discussion we will look at the (right-) knee angle data from several runners on a treadmill.

For a proof of the validity of our methodology we assume a decaying serial correlation structure for the errors (see Assumption (A4) in Section 4). In order to verify that this is a reasonable assumption for the data under consideration we estimate the lag k autocorrelation $\gamma_k(t, s) = \text{Cor}(X_0(t), X_k(s))$ between $X_0(t)$ and $X_k(s)$ by

$$\hat{\gamma}_k(t, s) := \frac{\sum_{j=1}^{n-k} (X_j(t) - \bar{X}(t))(X_{j+k}(s) - \bar{X}(s))}{\sqrt{\sum_{j=1}^{n-k} (X_j(t) - \bar{X}(t))^2 \sum_{j=1}^{n-k} (X_{j+k}(s) - \bar{X}(s))^2}}.$$

Exemplary, we display in Figure 6 the aggregation by the L^2 -norm $\|\hat{\gamma}\|_2$ of one runner for various lags. One can observe that the resulting function decays quite quickly but is substantially different from 0 for $k = 1, 2$ which validates our assumption.

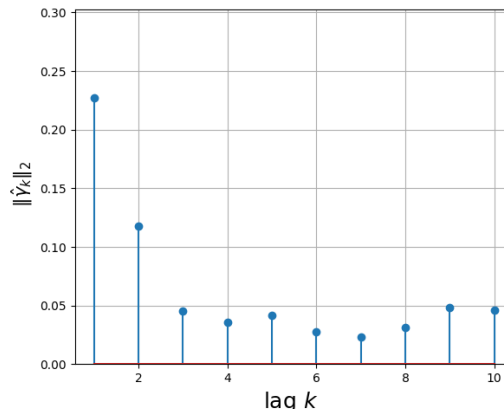


Figure 6: Variogram over lagged samples

In this type of application, the magnitude of adaptations of the biomechanical joints is an individual attribute of the respective runners (as seen in the examples in the following paragraphs). Consequently, the choice of the threshold Δ has to be individualised for each runner. We address this problem by estimating mean curves from the initial 5% and the final 5% of the curves and denote the corresponding estimates by $\hat{\mu}_{\text{initial}}$ and by $\hat{\mu}_{\text{final}}$. The threshold is then defined by $\Delta = \|\hat{\mu}_{\text{initial}} - \hat{\mu}_{\text{final}}\|_{\infty}/3$ as we expect the runners to go from rest phase to pre-fatigued and finally fatigued phases.

In Figure 7, we visualize the results of the methodology to detect relevant changes (denoted by crosses) due to fatigue for a particular runner. Notice that the densely collected functional data has no obvious jumps and fatigue detection for such a data requires us to use sophisticated change point detection techniques. For this particular runner with sample size $n = 1800$ the relevant difference threshold is $\Delta = 6$ and the first two change points detected by Algorithm 1 are relevant, implying a significant change (i.e., an increase) in the knee

angles at least up to 6 degrees. Comparing the mean curves from each consecutive segment in the bottom part of Figure 7, we obtain that the largest change is at the peak knee flexion which means more bending of the knee during the swing phase (when the corresponding foot is in the air). This is in agreement with prior studies, as in Zandbergen et al. (2023b), who also have reported this in their preliminary analysis of fatigue data. This increase in the knee flexion is attributed to decreased levels of stiffness in the runner during a fatigue protocol and is understood to be an attempt by runners to decrease the moment of inertia about the hip joint and could be attributed to a protection mechanism of the runner. Interestingly enough the second detected relevant change (at about 40% of the stride cycle) occurs when the corresponding foot makes contact with the ground and may be attributed to be the cause of higher oxygen-cost in the later stages of the run.

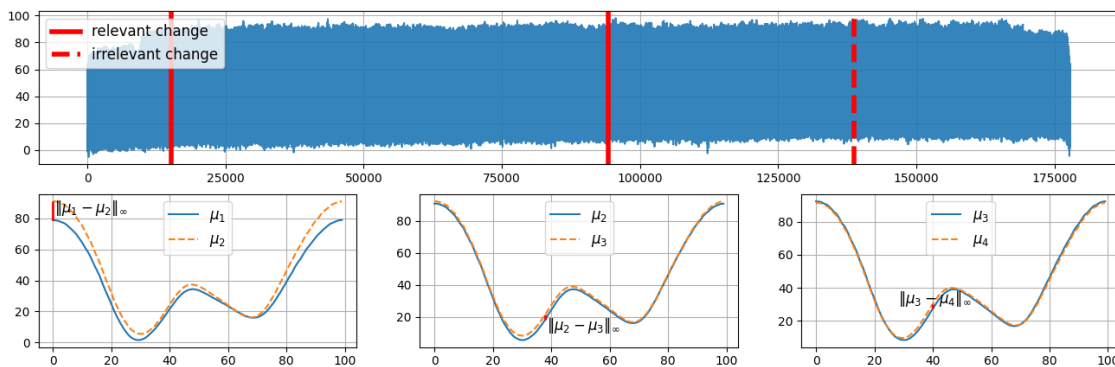


Figure 7: *Biomechanical knee angle data for a single runner in indoor setting. Upper part: The full functional time series with crosses depicting that two detected changes are relevant. Lower part: Mean curves on the different detected segments and maximum deviations marked by (red) vertical lines. The sample size for this runner is $n = 1800$.*

While the runner in Figure 7 shows an increased range of motion under fatigue conditions (an expected phenomenon) we display in Figure 8 the results for an alternative runner, with sample size $n = 1800$. Here, $\Delta = 5$ and Algorithm 2 identifies three relevant changes along with a reduced range of motion. At the first change point, the difference is picked up at peak knee flexion (captured at $\|\mu_1 - \mu_2\|_\infty$ in Figure 8) during the stance phase corresponding to the phase of contact of the foot with the ground. This inevitably leads to the ground reaction forces causing an increased load on the knees. The second and third changes (of size $\|\mu_2 - \mu_3\|_\infty$ and $\|\mu_3 - \mu_4\|_\infty$ respectively) point towards a reduction in the knee extension and flexion respectively. This is an interesting, albeit concerning change because it is contrary to observations for most runners, where one expects reduced stiffness and hence increased range of motion, see Apte et al. (2021). Such individual feedback on anomalies of the movement is valuable for future study of biomechanical data.

We conclude this section with a brief robustness study of Algorithm 2 with respect to the choice of the two tuning parameters, the block-length L in the bootstrap and the threshold ξ_n in the estimators of the extremal sets. For this purpose we apply the algorithm with different choices of these parameters to the Xsens data of a third runner. Here the sample size is $n = 1400$ and is chosen as $\Delta = 2.45$. Table 1 shows the results for different choices of the block length. We observe that the same change points are estimated for a wide range

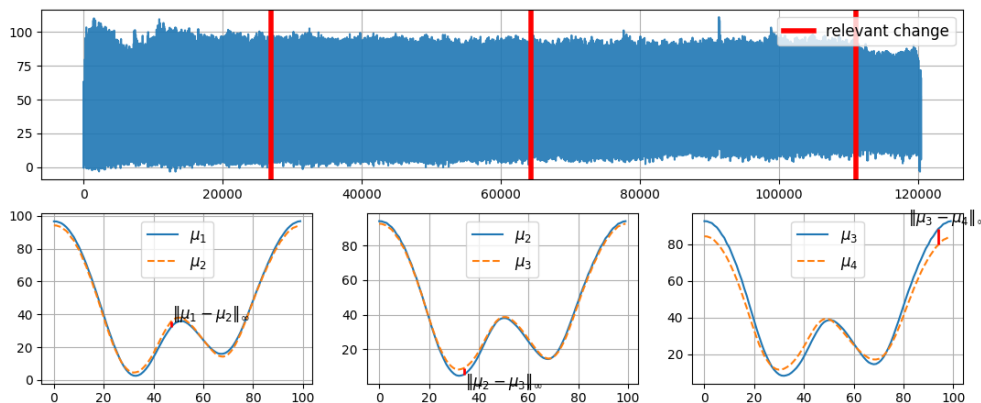


Figure 8: *Biomechanical knee angle data for an alternate runner in indoor setting showing interesting characteristics. Upper part: The full functional time series with crosses depicting that all detected changes are relevant. Lower part: Mean curves on the different detected segments and maximum deviations marked by (red) vertical lines. Sample size for this runner $n = 1205$.*

of the block length provided that this is not chosen too large. Similarly, we see from Table 2 that Algorithm 2 is rather robust with respect to the choice of ξ_n provided that it is not chosen too large (in that case binary segmentation fails to pick up some of the relevant change points) or too small (in that case the power of the procedure is diminished as the effective sample size of the intervals $[\hat{s}_{i-1}, \hat{s}_{i+1}]$ is reduced too much). Nevertheless, there is still a wide window of possible choices that produces the same change points and even in the more extreme cases the change points that are deemed relevant are consistent with the more moderate scenarios.

	$\alpha = 0.1$	$L = 3$	$L = 4$	$L = 5$	$L = 7$	$L = 9$	$L = 12$	$L = 15$
first change		526	526	526	526	526	526	526
second change		1112	1112	1112	1112	1112	1112	-
third change		-	1137	-	-	-	-	-
	$\alpha = 0.05$	$L = 3$	$L = 4$	$L = 5$	$L = 7$	$L = 9$	$L = 12$	$L = 15$
first change		526	526	526	526	526	-	-
second change		1112	1112	1112	1112	1112	-	-
third change		-	-	-	-	-	-	-

Table 1: Relevant changes in the knee angle data of single runner detected by Algorithm 2 with different block-lengths.

3.2.2 Marathon data

As an example for a rather uncontrolled environment we consider marathon data, which gives rise to deviations due to factors external from the runner's fatigue. On the other hand, runners in such data sets are typically far more experienced and changes and adaptations in their biomechanical data are fewer and are of a smaller size. Details on the data sets used

$\alpha = 0.1$	Binseg changes	Relevant changes
$\xi_n = 4.25$	[260, 526, 1112, 1137, 1163, 1185]	526, 1112, 1137
$\xi_n = 5.5$	[526, 1112, 1137, 1163, 1185]	526, 1112, 1137
$\xi_n = 6.1465$	[526, 1112, 1137, 1163, 1185]	526, 1112, 1137
$\xi_n = 7$	[526]	526
$\alpha = 0.05$	Binseg changes	Relevant changes
$\xi_n = 4.25$	[260, 526, 1112, 1137, 1163, 1185]	1112
$\xi_n = 5.5$	[526, 1112, 1137, 1163, 1185]	526, 1112, 1137
$\xi_n = 6.1465$	[526, 1112, 1137, 1163, 1185]	526, 1112, 1137
$\xi_n = 7$	[526]	526

Table 2: Robustness of multiple change point estimators with respect to the choice of ξ_n by Algorithm 2. Left part: estimated change points by binary segmentation (step 1). Right part: estimated relevant change points.

in this section, can be found in Zandbergen et al. (2023a). We choose Δ just as before in the sensor data example in Section 3.2.1. An illustration of our methodology for one of the runners is shown in Figure 9, where $\Delta = 3$. This runner, with a fairly large sample size of $n = 22000$, shows an initial relevant adjustment to (perceived-) fatigue in the marathon followed by an adjustment that is below the relevant size. Finally towards the end of the run, another relevant change to the knee movement occurs. We recover that both the relevant adjustments are in the flexion of the knee when the foot is in the air with an increase in the range of motion indicating reduced stiffness. Finally, the irrelevant change still marks the tendency of the increase in flexion of the knee angle at this point (stance phase, foot is in contact with the ground) during fatigue situation but is just not significant in this particular runner data and therefore not relevant for further analysis only in this case. Note that this is in contrast with some inexperienced runners where changes in the biomechanical data is also captured at this point of the stance phase; see Figure 8, and Maas et al. (2018) for a further discussion on such increased kinematic changes in novice runners. This example reiterates the usefulness of looking for relevant changes and not just at all changes in the data.

4 Theoretical analysis

In this section we establish the validity of our approach. For the theoretical analysis, we recall the definition of the triangular array in (2.1), use the notations $X_{n,j}$, $\epsilon_{n,j}$, $\mu_{n,j}$ etc. to emphasize the dependence on n and make the following assumptions.

(A1) The error process $\{\epsilon_{n,j} | j = 1, \dots, n\}_{n \in \mathbb{N}}$ is a triangular-array of centered $C([0, 1])$ -valued random variables (i.e. for fixed n the process $(\epsilon_{n,1}, \dots, \epsilon_{n,n})$ is stationary and $\mathbb{E}[\epsilon_{n,j}] = 0$).

(A2) There exists a constant K such that for all $j \in \mathbb{N}$ we have

$$\mathbb{E}[\|\epsilon_{n,j}\|^{2+\nu}] \leq K, \quad \mathbb{E}[\|\epsilon_{n,j}\|^J] < \infty$$

for some $\nu > 0$ and some even integer $J \geq 2$.

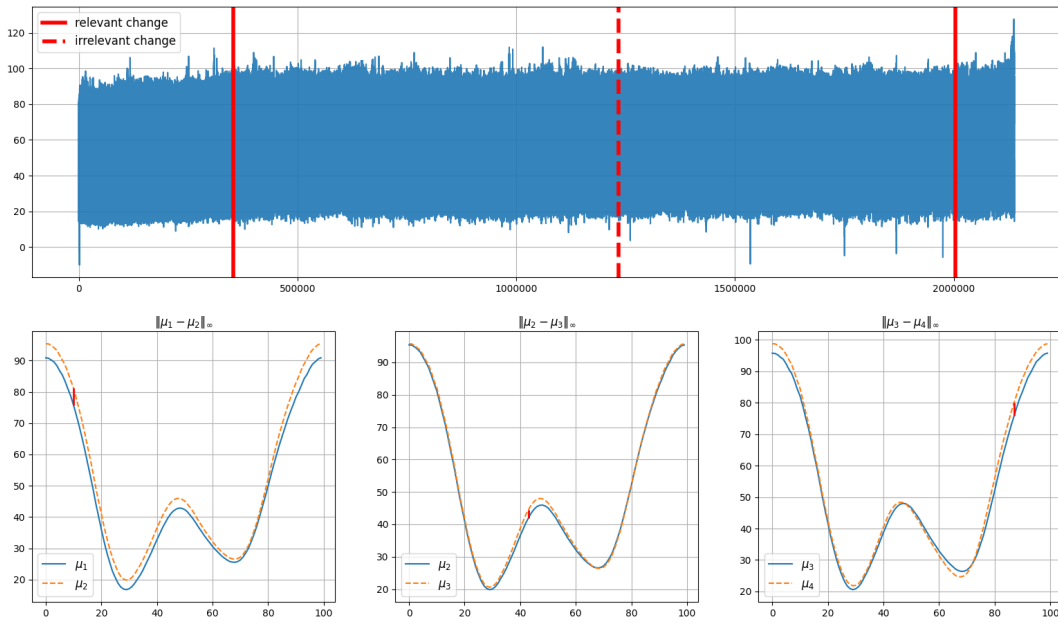


Figure 9: *Biomechanical knee angle data of single marathon runner. Upper part: The full functional time series with two relevant changes (denoted by crosses) and one irrelevant change. Lower part: Mean curves on the different detected segments and maximum deviations marked by (red) vertical lines. The sample size for this runner is $n = 22000$.*

(A3) There exists some $\theta \in (0, 1]$ with $\theta J > 1$ and a non-negative real random variable M with $\mathbb{E}[M^J] < \infty$ such that for any $n \in \mathbb{N}$ and $j = 1, \dots, n$ the inequality

$$|X_{n,j}(t) - X_{n,j}(t')| \leq M|t - t'|^\theta$$

holds almost surely. Here J is the same constant as in (A1).

(A4) $(\epsilon_{n,j}, j \in \mathbb{N})$ is ϕ -mixing with mixing coefficients satisfying for some $\bar{\tau} \in (1/(2+2\nu), 1/2)$ the condition

$$\sum_{k=1}^{\infty} k^{1/(1/2-\bar{\tau})} \phi(k)^{1/2} < \infty, \quad \sum_{k=1}^{\infty} (k+1)^{J/2-1} \phi(k)^{1/J} < \infty.$$

Our first result establishes the consistency of the estimator \hat{m} of the number of change points and of the estimators $\hat{s}_1, \dots, \hat{s}_{\hat{m}}$ of the location of the change points defined by Algorithm 1. The proof is deferred to the appendix.

Theorem 4.1 (consistency of Algorithm 1). *Suppose that Assumptions (A1), (A2) and (A4) hold and that*

$$\frac{\log^{1/2}(n)}{\xi_n} + \frac{\xi_n}{\sqrt{n}} = o(1).$$

as $n \rightarrow \infty$. Then

$$\mathbb{P}\left(\hat{m} = m, \max_{1 \leq i \leq m} |\hat{s}_i - s_i| \leq \log(n)/n\right) \rightarrow 1.$$

Theorem 4.2. *Suppose that assumptions (A1) - (A4) hold with $\nu \geq 2$ in (A1). If additionally $L = n^\beta$ with $\beta \in [1/5, 2/7]$ such that*

$$(\beta(2 + \nu) + 1)/(2 + 2\nu) < \bar{\tau} < 1/2$$

in Assumption (A4) we obtain that the estimator of the set of relevant change points is consistent in the following sense.

(i) If $S_{\text{rel}} = \emptyset$, we have

$$\liminf_{n \rightarrow \infty} \mathbb{P}(\hat{S}_{\text{rel}} = \emptyset) \geq 1 - \alpha.$$

Moreover, if additionally $\max_{1 \leq i \leq m} \|\mu_{i+1} - \mu_i\|_\infty < \Delta$ this can be strengthened to

$$\lim_{n \rightarrow \infty} \mathbb{P}(\hat{S}_{\text{rel}} = \emptyset) = 1 \tag{4.1}$$

(ii) We have

$$\lim_{n \rightarrow \infty} \mathbb{P}(S_{\text{rel}} \subset (\hat{S}_{\text{rel}} + \log(n)/n)) = 1 \tag{4.2}$$

as well as

$$\liminf_{n \rightarrow \infty} \mathbb{P}(\hat{S}_{\text{rel}} \subset (S_{\text{rel}} + \log(n)/n)) \geq 1 - \alpha. \tag{4.3}$$

The latter also can be strengthened to

$$\lim_{n \rightarrow \infty} \mathbb{P}(\hat{S}_{\text{rel}} \subset (S_{\text{rel}} + \log(n)/n)) = 1 \tag{4.4}$$

whenever $\max_{1 \leq i \leq m, s_i \notin S_{\text{rel}}} \|\mu_{i+1} - \mu_i\|_\infty < \Delta$.

Remark 4.1.

- (a) From a theoretical point of view our results can be extended to the case, where the mean functions on the different segments vary with n , that is $\mu_j = \mu_j^{(n)}$ ($j = 1, \dots, m$). In this case Theorem 4.1 and 4.2 remain valid under the additional assumptions:

$$\begin{aligned} \min_{n \in \mathbb{N}} \min_{1 \leq j \leq m} \|\mu_j^{(n)} - \mu_{j-1}^{(n)}\|_\infty &\geq \eta > 0, \\ \max_{n \in \mathbb{N}} \max_{0 \leq j \leq m} \|\mu_j^{(n)}\|_\infty &< \infty, \\ \sqrt{n} \left(\min_{1 \leq i \leq m, s_i \in S_{\text{rel}}} \|\mu_{i+1}^{(n)} - \mu_i^{(n)}\|_\infty - \Delta \right) &\rightarrow \infty. \end{aligned}$$

For the additional statements (4.1) and (4.4) in Theorem 4.1 and 4.2 we further require

$$\begin{aligned} \max_{n \in \mathbb{N}} \max_{1 \leq i \leq m} \|\mu_{i+1} - \mu_i\|_\infty &< \Delta, \\ \max_{n \in \mathbb{N}} \max_{1 \leq i \leq m, s_i \notin S_{\text{rel}}} \|\mu_{i+1} - \mu_i\|_\infty &< \Delta, \end{aligned}$$

respectively.

- (b) All results presented in this also hold for sufficiently densely observed functional data. In this case additional assumptions on the smoothness of the trajectories positively influences the performance of our method as there is a trade off between how densely the data is observed and how well we can interpolate to obtain estimates of the functions.
- (c) It is also possible to consider a sequence of nominal levels, say $\alpha = \alpha_n$, in Theorem 4.2, such that α_n that converges to 0 at a polynomial rate. In this case we have instead of (4.2) and (4.3)

$$\lim_{n \rightarrow \infty} \mathbb{P}(S_{\text{rel}} = \hat{S}_{\text{rel}}) = 1, f$$

whenever

$$\frac{\sqrt{n}}{\log(n)} \left(\min_{1 \leq i \leq m, s_i \in S_{\text{rel}}} \|\mu_{i+1}^{(n)} - \mu_i^{(n)}\|_\infty - \Delta \right) \rightarrow \infty.$$

This observation is a consequence of the fact that the statistic $D(\mathcal{E})$ in (2.10) is bounded by $\max_{1 \leq i \leq m} \|\mathbb{W}_i\|_\infty$ where the random variables \mathbb{W}_i have the same distribution as the process \mathbb{W} in (2.10). By Fernique's Theorem (see Fernique, 1975) each random variable $\|\mathbb{W}_i\|_\infty$ has subgaussian tails. This implies at most logarithmic growth of the quantiles of $D(\mathcal{E})$ in $1/\alpha$.

- (d) We note that the localization rates obtained in Theorem 4.1 are minimax optimal up to a logarithmic factor (see the discussion in section 1.4 of Verzelen et al. (2023)).

Ethics statement: The ethics committee at the university of Twente., (Ethical Committee EEMCS (EC-CIS), University of Twente, ref.: RP 2022-20) approved the experimental protocol of this study.

Additional resources : Data may be made available on reasonable request. The source code used in this paper is available on github [rupsabasu2020/multiple_relevant_CP](https://github.com/rupsabasu2020/multiple_relevant_CP).

Acknowledgments This work was partially supported by the Deutsche Forschungsgemeinschaft: DFG Research unit 5381 *Mathematical Statistics in the Information Age*, project

number 460867398 and by the project titled: Modeling functional time series with dynamic factor structures and points of impact”, with project number 511905296. We thank the team of *Sports, Data, and Interaction*³, in particular Robbert van Middelaar and Aswin Balasubramaniam for meticulously collecting, pre-processing and providing the data used in this work and Bram Kohlen for helping refine the implementation of Algorithm 1 on python.

References

- Apte, S., Prigent, G., Stögl, T., Martínez, A., Snyder, C., Gremeaux-Bader, V., and Aminian, K. (2021). Biomechanical response of the lower extremity to running-induced acute fatigue: a systematic review. *Frontiers in Physiology*, 12:646042.
- Aston, J. A. D. and Kirch, C. (2012). Evaluating stationarity via change-point alternatives with applications to fMRI data. *The Annals of Applied Statistics*, 6(4):1906 – 1948.
- Aue, A., Gabrys, R., Horváth, L., and Kokoszka, P. (2009). Estimation of a change-point in the mean function of functional data. *Journal of Multivariate Analysis*, 100(10):2254–2269.
- Aue, A., Rice, G., and Sönmez, O. (2018). Detecting and dating structural breaks in functional data without dimension reduction. *Journal of the Royal Statistical Society Series B: Statistical Methodology*, 80(3):509–529.
- Baranowski, R., Chen, Y., and Fryzlewicz, P. (2019). Narrowest-Over-Threshold Detection of Multiple Change Points and Change-Point-Like Features. *Journal of the Royal Statistical Society Series B: Statistical Methodology*, 81(3):649–672.
- Berkes, I., Gabrys, R., Horváth, L., and Kokoszka, P. (2009). Detecting Changes in the Mean of Functional Observations. *Journal of the Royal Statistical Society Series B: Statistical Methodology*, 71(5):927–946.
- Bucchia, B. and Wendler, M. (2017). Change-point detection and bootstrap for hilbert space valued random fields. *Journal of Multivariate Analysis*, 155:344–368.
- Cárcamo, J., Cuevas, A., and Rodríguez, L.-A. (2020). Directional differentiability for supremum-type functionals: Statistical applications. *Bernoulli*, 26(3):2143 – 2175.
- Chiou, J.-M., Chen, Y.-T., and Hsing, T. (2019). Identifying multiple changes for a functional data sequence with application to freeway traffic segmentation. *The Annals of Applied Statistics*, 13:1430–1463.
- Cho, H. (2016). Change-point detection in panel data via double CUSUM statistic. *Electronic Journal of Statistics*, 10(2):2000 – 2038.
- Cho, H. and Fryzlewicz, P. (2014). Multiple-Change-Point Detection for High Dimensional Time Series via Sparsified Binary Segmentation. *Journal of the Royal Statistical Society Series B: Statistical Methodology*, 77(2):475–507.
- Detle, H., Eckle, T., and Vetter, M. (2020a). Multiscale change point detection for dependent data. *Scandinavian Journal of Statistics*, 47(4):1243–1274.

³<http://www.sports-data-interaction.com>

- Dette, H., Kokot, K., and Aue, A. (2020b). Functional data analysis in the Banach space of continuous functions. *The Annals of Statistics*, 48(2):1168 – 1192.
- Dette, H., Kokot, K., and Volgushev, S. (2020c). Testing Relevant Hypotheses in Functional Time Series via Self-Normalization. *Journal of the Royal Statistical Society Series B: Statistical Methodology*, 82(3):629–660.
- Dette, H. and Kutta, T. (2021). Detecting structural breaks in eigensystems of functional time series. *Electronic Journal of Statistics*, 15(1):944 – 983.
- Eichinger, B. and Kirch, C. (2018). A MOSUM procedure for the estimation of multiple random change points. *Bernoulli*, 24(1):526 – 564.
- Fernique, X. (1975). Regularite des trajectoires des fonctions aleatoires gaussiennes. In Hennequin, P. L., editor, *Ecole d’Eté de Probabilités de Saint-Flour IV—1974*, pages 1–96, Berlin, Heidelberg. Springer Berlin Heidelberg.
- Frick, K., Munk, A., and Sieling, H. (2014). Multiscale change point inference. *Journal of the Royal Statistical Society Series B: Statistical Methodology*, 76(3):495–580.
- Fryzlewicz, P. (2014). Wild binary segmentation for multiple change-point detection. *The Annals of Statistics*, 42(6):2243 – 2281.
- Harris, T., Li, B., and Tucker, J. D. (2022). Scalable multiple changepoint detection for functional data sequences. *Environmetrics*, 33(2):e2710.
- Horváth, L., Kokoszka, P., and Rice, G. (2014). Testing stationarity of functional time series. *Journal of Econometrics*, 179(1):66–82.
- Killick, R., Fearnhead, P., and Eckley, I. A. (2012). Optimal detection of changepoints with a linear computational cost. *Journal of the American Statistical Association*, 107(500):1590–1598.
- Kovács, S., Bühlmann, P., Li, H., and Munk, A. (2023). Seeded binary segmentation: a general methodology for fast and optimal changepoint detection. *Biometrika*, 110(1):249–256.
- Li, H., Guo, Q., and Munk, A. (2017). Multiscale change-point segmentation: Beyond step functions. *Electronic Journal of Statistics*, 13.
- Maas, E., De Bie, J., Vanfleteren, R., Hoogkamer, W., and Vanwanseele, B. (2018). Novice runners show greater changes in kinematics with fatigue compared with competitive runners. *Sports Biomechanics*, 17(3):350–360.
- Madrid Padilla, C. M., Wang, D., Zhao, Z., and Yu, Y. (2022). Change-point detection for sparse and dense functional data in general dimensions. In Koyejo, S., Mohamed, S., Agarwal, A., Belgrave, D., Cho, K., and Oh, A., editors, *Advances in Neural Information Processing Systems*, volume 35, pages 37121–37133. Curran Associates, Inc.
- Maidstone, R., Hocking, T., Rigai, G., and Fearnhead, P. (2017). On optimal multiple changepoint algorithms for large data. *Statistics and Computing*, 27(2):519–533.

- Padilla, O. H. M., Yu, Y., Wang, D., and Rinaldo, A. (2021). Optimal nonparametric multivariate change point detection and localization. *IEEE Transactions on Information Theory*, 68(3):1922–1944.
- Rice, G. and Shang, H. L. (2017). A plug-in bandwidth selection procedure for long-run covariance estimation with stationary functional time series. *Journal of Time Series Analysis*, 38(4):591–609.
- Rice, G. and Zhang, C. (2022). Consistency of binary segmentation for multiple change-point estimation with functional data. *Statistics & Probability Letters*, 180:109228.
- Schepers, M., Giuberti, M., Bellusci, G., et al. (2018). Xsens mvn: Consistent tracking of human motion using inertial sensing. *Xsens Technol*, 1(8).
- Shapiro, O., Tewes, J., and Wendler, M. (2016). Sequential block bootstrap in a hilbert space with application to change point analysis. *The Canadian Journal of Statistics / La Revue Canadienne de Statistique*, 44(3):300–322.
- Stoehr, C., Aston, J. A. D., and Kirch, C. (2021). Detecting changes in the covariance structure of functional time series with application to fmri data. *Econometrics and Statistics*, 18:44–62.
- Tukey, J. W. (1991). The philosophy of multiple comparisons. *Statistical Science*, 6(1):100–116.
- Verzelen, N., Fromont, M., Lerasle, M., and Reynaud-Bouret, P. (2023). Optimal change-point detection and localization. *The Annals of Statistics*, 51(4):1586 – 1610.
- Vostrikova, L. Y. (1981). Detecting “disorder” in multidimensional random processes. *Dokl. Akad. Nauk SSSR*, 259(2):270–274.
- Wang, D., Yu, Y., and Rinaldo, A. (2020). Univariate mean change point detection: Penalization, CUSUM and optimality. *Electronic Journal of Statistics*, 14(1):1917 – 1961.
- Wang, T. and Samworth, R. J. (2017). High Dimensional Change Point Estimation via Sparse Projection. *Journal of the Royal Statistical Society Series B: Statistical Methodology*, 80(1):57–83.
- Xuejun, W., Shuhe, H., Yan, S., and Wenzhi, Y. (2009). Moment inequality for-mixing sequences and its applications. *Journal of Inequalities and Applications*, 2009(1):379743.
- Zandbergen, M. A., Buurke, J. H., Veltink, P. H., and Reenalda, J. (2023a). Quantifying and correcting for speed and stride frequency effects on running mechanics in fatiguing outdoor running. *Frontiers in Sports and Active Living*, 5:1085513.
- Zandbergen, M. A., Marotta, L., Bulthuis, R., Buurke, J. H., Veltink, P. H., and Reenalda, J. (2023b). Effects of level running-induced fatigue on running kinematics: A systematic review and meta-analysis. *Gait & Posture*, 99:60–75.

5 Appendix

6 Supplement

In this appendix we represent the proofs of the theoretical results in Section 4. Recall that $\hat{S} = \{\hat{s}_1, \dots, \hat{s}_m\}$ is the set of estimated change points. Throughout this section $\|\cdot\|_2$ always refers to the L^2 -norm.

6.1 Proof of Theorem 4.1 (consistency of BINSEG)

The proof follows from Theorem 2.2 in Rice and Zhang (2022). To apply this result we need to verify the Assumption 2 - 5 of this reference. We begin with Assumption 3.

Let ω_j denote the modulus of continuity of the function $\mu_j - \mu_{j-1}$ and note that $|\mu_j(t) - \mu_{j-1}(t')| \leq \omega_j(|t - t'|)$. As $\omega_j(0) = 0$, ω_j is continuous, increasing and $\mu_j - \mu_{j-1} \neq 0$, there exists a positive constant $\delta_j > 0$ such that $\omega_j(\delta_j) = \|\mu_j - \mu_{j-1}\|_\infty / 2$. Thus we can find an interval $I \subset [0, 1]$ with length at least δ_j such that $|\mu_j(t) - \mu_{j-1}(t')| > \|\mu_j - \mu_{j-1}\|_\infty / 2$ for all $t, t' \in I$. As there are only finitely many of these differences it follows that

$$\min_{1 \leq j \leq m} \|\mu_j - \mu_{j-1}\|_2 \geq \eta := \min_{1 \leq j \leq m} \|\mu_j - \mu_{j-1}\|_\infty \cdot \min_{1 \leq j \leq m} \delta_j .$$

Therefore, Assumption 3 in Rice and Zhang (2022) is satisfied. Assumption 4 is immediate as m is fixed. Assumption 5 follows from the fact that $\|\mu_j\|_\infty < \infty$ in combination with $\|\cdot\|_2 \leq \|\cdot\|_\infty$. Finally, Assumption 2 is a consequence of the following Lemma.

Lemma 6.1. *Assume that $(\epsilon_i)_{i \in \mathbb{N}}$ is a stationary sequence with $\mathbb{E}[\|\epsilon_i\|_2] \leq K$ such that $\sum_{n=1}^\infty \phi(n)^{1/2} < \infty$. Then we obtain for the mean $\bar{\epsilon}_k = \frac{1}{k} \sum_{i=1}^k \epsilon_i$.*

$$\mathbb{P}\left(\max_{1 \leq k \leq n} \sqrt{k} \|\bar{\epsilon}_k\|_2 > x\right) \leq C \log(n) x^{-2}$$

where C depends only on K and $(\phi(n))_{n \in \mathbb{N}}$.

Proof. Using similar arguments as in the proof of Lemma B.1 in the online supplement to Aue et al. (2018) we obtain

$$\mathbb{P}\left(\max_{1 \leq k \leq n} \sqrt{k} \|\bar{\epsilon}_k\|_2 > x\right) \leq \sum_{j=1}^{c \log(n)} 2^{-(j-1)} x^{-2} \mathbb{E}\left[\left(\max_{1 \leq k \leq 2^j} \left\| \sum_{i=1}^k \epsilon_i \right\|_2\right)^2\right]$$

(note that this estimate does not depend on the dependence structure of the random variables). Observe that $(\epsilon_i)_{i \in \mathbb{N}}$ ϕ -mixing implies that $(\|\epsilon_i\|_2)_{i \in \mathbb{N}}$ is ϕ -mixing with mixing coefficients at most as large as those of $(\epsilon_i)_{i \in \mathbb{N}}$. In particular we may use Theorem 2.1 from Xuejun et al. (2009) to obtain

$$\mathbb{E}\left[\left(\max_{1 \leq k \leq 2^j} \left\| \sum_{i=1}^k \epsilon_i \right\|_2\right)^2\right] \leq 2^j K_0,$$

where K_0 depends only on K and $(\phi(n))_{n \in \mathbb{N}}$, this then yields

$$\mathbb{P}\left(\max_{1 \leq k \leq n} \sqrt{k} \|\bar{\epsilon}_k\|_2 > x\right) \leq 2cK_0 \log(n) x^{-2} .$$

□

6.2 Some preliminary steps for the proof of Theorem 4.2

In this section we will prove a preliminary result regarding a test for the hypothesis that there exists at least one *structural break of relevant size* in the sequence of data $X_{n,1}, X_{n,2}, \dots, X_{n,n}$, i.e we consider the hypotheses

$$H_0 : \max_{1 \leq k \leq m} \|\mu_k - \mu_{k-1}\|_\infty \leq \Delta \quad \text{vs.} \quad H_1 : \max_{1 \leq k \leq m} \|\mu_k - \mu_{k-1}\|_\infty > \Delta. \quad (6.1)$$

In fact it turns out that the decision rule

$$\hat{T}_n > q_{1-\alpha}^*$$

defines a consistent and asymptotic level α test. Besides of being of interest on its own, this result is the basis for establishing the consistency of Algorithm 2 with respect to the estimation of the relevant change points (see Theorem 4.2 below).

Theorem 6.1. *Let $q_{1-\alpha}^*$ be the $(1 - \alpha)$ -quantile obtained in the course of Algorithm 2, and suppose that assumptions (A1) - (A4) hold with $\nu \geq 2$ in (A1). If additionally $L = n^\beta$ with $\beta \in [1/5, 2/7]$ such that*

$$(\beta(2 + \nu) + 1)/(2 + 2\nu) < \bar{\tau} < 1/2$$

in Assumption (A4), the following statements hold true.

(i) *Under the null hypothesis of no relevant change point we have*

$$\limsup_{n \rightarrow \infty} \mathbb{P}(\hat{T}_n > q_{1-\alpha}^*) \leq \alpha,$$

with equality whenever $\|\mu_i - \mu_{i-1}\|_\infty = \Delta$ for all $i = 1, \dots, m$.

(ii) *Whenever $(\max_{1 \leq i \leq m} \|\mu_i - \mu_{i-1}\| - \Delta) > 0$ we have*

$$\lim_{n \rightarrow \infty} \mathbb{P}(\hat{T}_n > q_{1-\alpha}^*) = 1.$$

The proof of Theorem 6.1 consists of three steps (which will be proved below). We first derive the asymptotic distribution of the statistic \hat{D}_n defined in (2.10).

Theorem 6.2 (weak convergence of \hat{D}_n). *Under the assumptions of Theorem 6.1 we have $\hat{D}_n \xrightarrow{D} D(\mathcal{E})$, where \hat{D}_n and $D(\mathcal{E})$ are defined in (2.10).*

Next we derive a (consistent) and asymptotic level α for the hypotheses (6.1) of no relevant change point using the statistic \hat{T}_n defined in (2.5) and the $(1 - \alpha)$ -quantile of the random variable $D(\mathcal{E})$ in (2.10) (note that this test is not feasible as the quantile depends in a complicated manner on the extremal sets and the dependence structure of the process).

Theorem 6.3. *Let $q_{1-\alpha}$ denote the $(1 - \alpha)$ quantile of $D(\mathcal{E})$. Under the Assumptions of Theorem 6.1 we have*

(i) *Under the null hypothesis it holds that $\limsup_{n \rightarrow \infty} \mathbb{P}(\hat{T}_n > q_{1-\alpha}) \leq \alpha$ with equality whenever $\|\mu_i - \mu_{i-1}\|_\infty = \Delta$ for all $i = 1, \dots, m$.*

(ii) $\lim_{n \rightarrow \infty} \mathbb{P}(\hat{T}_n > q_{1-\alpha}) = 1$ whenever $(\max_{1 \leq i \leq m} \|\mu_i - \mu_{i-1}\|_\infty - \Delta) > 0$.

Finally we show that the multiplier bootstrap proposed in Algorithm 2 produces asymptotically the same distribution as the statistic \hat{D}_n in Theorem 6.2. For this purpose we show the following result.

Theorem 6.4. *Under Assumptions of Theorem (6.1) we have*

$$(\hat{D}_n, \hat{T}_n^{(1)}, \dots, \hat{T}_n^{(R)}) \xrightarrow{\mathcal{D}} (D(\mathcal{E}), D^{(1)}(\mathcal{E}), \dots, D^{(R)}(\mathcal{E})),$$

where $D(\mathcal{E}), D^{(1)}(\mathcal{E}), \dots, D^{(R)}(\mathcal{E})$ are independent copies of $D(\mathcal{E})$.

The assertion of Theorem 6.1 now follows combining Theorem 6.2 - 6.4.

6.2.1 Proof of Theorem 6.2

Throughout this section the symbol \rightsquigarrow denotes weak convergence in the space of bounded functions on a compact rectangular region, which will always be clear from the context. We now have the following result.

Theorem 6.5.

$$\left\{ \sqrt{n_i} \left(\hat{U}_{\hat{k}_{i-1}, \hat{k}_{i+1}}(\hat{h}^{-1}(s), t) - (s \wedge \hat{h}_i(s_i) - s \hat{h}_i(s_i))(\mu_{i+1}(t) - \mu_i(t)) \right) \right\}_{(s,t) \in [0,1]^2} \rightsquigarrow \{\mathbb{W}(s, t)\}_{(s,t) \in [0,1]^2},$$

where \mathbb{W} is a centered Gaussian process on $[0, 1]^2$ with covariance structure

$$\text{Cov}(\mathbb{W}(s, t), \mathbb{W}(s', t')) = (s \wedge s' - ss') \sum_{i=-\infty}^{\infty} \text{Cov}(\epsilon_{n,0}(t), \epsilon_{n,i}(t)).$$

The latter definition does not depend on the choice of j by the row-wise stationarity of the error process array. The convergence also holds jointly with respect to $1 \leq i \leq m$.

Proof. Let $k_i = \lfloor ns_i \rfloor$ ($i = 0, \dots, m+1$) and consider the process

$$\begin{aligned} \hat{U}_{k_{i-1}, k_{i+1}}(h^{-1}(s), t) &= \frac{1}{n_i} \left(\sum_{j=k_{i-1}+1}^{\lfloor h_i^{-1}(s) n_i \rfloor} X_{n,j}(t) + n_i \left(h^{-1}(s) - \frac{\lfloor h^{-1}(s) n_i \rfloor}{n_i} \right) X_{n, k_{i+1}}(t) \right. \\ &\quad \left. - s \sum_{j=k_{i-1}+1}^{k_{i+1}} X_{n,j}(t) \right), \end{aligned}$$

on $[0, 1]^2$, where $n_i = n(s_{i+1} - s_{i-1})$. By the proof of Theorem 4.1 from Dette et al. (2020b) it follows that the statement of Theorem 6.5 holds if $\hat{U}_{\hat{k}_{i-1}, \hat{k}_{i+1}}(\hat{h}^{-1}(s), t)$ is replaced by $\hat{U}_{k_{i-1}, k_{i+1}}(h^{-1}(s), t)$. By equation (6.2) from the proof of Lemma 6.2 the difference

$$\hat{U}_{\hat{k}_{i-1}, \hat{k}_{i+1}}(\hat{h}^{-1}(s), t) - \hat{U}_{k_{i-1}, k_{i+1}}(h^{-1}(s), t)$$

is of order $o_{\mathbb{P}}(1/\sqrt{n})$ uniformly with respect to $s, t \in [0, 1]$. Therefore the first assertion follows. The second assertion is a consequence of the weak convergence of the finite dimensional distributions of the vector $(\hat{U}_{0, k_2}, \dots, \hat{U}_{k_{m-1}, 1})^\top$, which can be verified by tedious but straightforward calculations (note that equicontinuity is obvious as each component is equicontinuous). \square

To continue with the proof of Theorem 6.2 define

$$D_n := \max_{1 \leq i \leq m} \left\{ \sqrt{n_i} (M_{n,i} - h_i(s_i)(1 - h_i(s_i)) \|\mu_i - \mu_{i-1}\|_\infty) \right\}$$

where $M_{n,i}$ is obtained from $\hat{M}_{n,i}$ by replacing the estimates \hat{s}_i by s_i . Consequently, D_n is the analog of \hat{D}_n in (2.10), where the estimates \hat{s}_i have been replaced by the unknown change points. As each $M_{n,i}$ is a supremum taken over a fixed interval we can apply the delta method for directionally Hadamard differentiable functions (see Cárcamo et al., 2020, Corollary 2.3) and obtain from Theorem 6.5 that

$$\begin{aligned} & \left\{ \sqrt{n_i} (M_{n,i} - h_i(s_i)(1 - h_i(s_i)) \|\mu_i - \mu_{i-1}\|_\infty) \right\}_{i=1, \dots, m} \\ & \xrightarrow{\mathcal{D}} \max \left\{ \sup_{t \in \mathcal{E}_i^+} \mathbb{W}(h_i(s_i), t), \sup_{t \in \mathcal{E}_i^-} -\mathbb{W}(h_i(s_i), t) \right\}. \end{aligned}$$

By the continuous mapping theorem we get $D_n \xrightarrow{\mathcal{D}} D(\mathcal{E})$. The proof of Theorem 6.2 is completed by an application of Lemma 6.2, which shows that we can replace each $M_{n,i}$ by $\hat{M}_{n,i}$, yielding $\hat{D}_n \xrightarrow{\mathcal{D}} D(\mathcal{E})$.

6.2.2 Proof of Theorem 6.3

The first part follows directly from Theorem 6.2 using the inequality $\hat{D}_n \leq \hat{T}_n$ which holds under the null hypothesis. For the second part we first observe that $\|\mu_i - \mu_{i-1}\|_\infty > \Delta$ for at least one $i \in \{1, \dots, m\}$. We denote the index with the largest jump size (with respect to the sup-norm) by i_0 . Recalling the definition of $\hat{T}_{n,i}$ in (2.4) and $D_{n,i}$ in (2.9) we have

$$\hat{T}_n \geq \hat{T}_{n,i_0} = D_{n,i_0} + \hat{h}_i(\hat{s}_{i_0})(1 - \hat{h}_i(\hat{s}_{i_0})) (\|\mu_{i_0} - \mu_{i_0-1}\|_\infty - \Delta).$$

By Theorem 6.2 the sequence $(D_{n,i_0})_{n \in \mathbb{N}}$ is tight, the right hand side of the preceding equation thus diverges to positive infinity. As the quantile $q_{1-\alpha}$ is a bounded quantity the theorem follows.

6.2.3 Proof of Theorem 6.4

Recall the definition of $\hat{U}_{l,r}$ in (2.3) and define $M_{n,i} = \|\hat{U}_{k_{i-1}, k_{i+1}}(h_i^{-1}(s), t)\|_\infty$ and $\hat{M}_{n,i} = \|\hat{U}_{\hat{k}_{i-1}, \hat{k}_{i+1}}(\hat{h}^{-1}(s), t)\|_\infty$. The proof follows directly from the following two statements.

Lemma 6.2. *Under the assumptions of Theorem 6.4 we have $\sqrt{n_i}(M_{n,i} - \hat{M}_{n,i}) = o_{\mathbb{P}}(1)$.*

Proof. It follows from Theorem 4.1 that $|\hat{s}_i - s_i| \leq \log(n)/n$ holds with high probability. We have

$$\begin{aligned} & \sqrt{n_i} (\hat{U}_{k_{i-1}, k_{i+1}}(h_i^{-1}(s), t) - \hat{U}_{\hat{k}_{i-1}, \hat{k}_{i+1}}(\hat{h}^{-1}(\tilde{s}), t)) \\ & = \frac{1}{\sqrt{n}} \left(\sum_{j=\lfloor sn \rfloor + 1}^{\lfloor \tilde{s}n \rfloor} X_{n,j}(t) + n_i \left(s - \frac{\lfloor sn \rfloor}{n_i} \right) X_{n, s_{i+1}}(t) \right. \\ & \quad \left. - \hat{n}_i \left(\tilde{s} - \frac{\lfloor \tilde{s}n \rfloor}{\hat{n}_i} \right) X_{n, \hat{s}_{i+1}}(t) - (h_i(s) - \hat{h}_i(\tilde{s})) \sum_{j=k_{i-1}+1}^{k_{i+1}} X_{n,j}(t) \right) + o_{\mathbb{P}}(1) \\ & = \frac{1}{\sqrt{n_i}} \sum_{j=\lfloor sn \rfloor}^{\lfloor \tilde{s}n \rfloor} X_{n,j}(t) + o_{\mathbb{P}}(1) = \frac{1}{\sqrt{n_i}} \sum_{j=\lfloor sn \rfloor}^{\lfloor \tilde{s}n \rfloor} \epsilon_{n,j}(t) + o_{\mathbb{P}}(1) \end{aligned}$$

uniformly with respect to $t \in [0, 1]$ and all $s < \tilde{s}$ with $\sqrt{n}|s - \tilde{s}| \leq \log(n)/\sqrt{n}$. An application of Markov's inequality then yields

$$\mathbb{P}\left(\sqrt{n_i} \sup_{t \in [0, 1]} \sup_{|s - \tilde{s}| \leq \frac{\log(n)}{n}} \left| \hat{U}_{k_{i-1}, k_{i+1}}(h_i^{-1}(s), t) - \hat{U}_{\hat{k}_{i-1}, \hat{k}_{i+1}}(\hat{h}^{-1}(\tilde{s}), t) \right| > x\right) \leq 2K \frac{\log n}{x} + o(1) = o(1) \quad (6.2)$$

Finally we observe that

$$\begin{aligned} & \sqrt{n} \left(\left\| \hat{U}_{k_{i-1}, k_{i+1}}(h_i^{-1}(s), t) \right\|_{\infty} - \left\| \hat{U}_{\hat{k}_{i-1}, \hat{k}_{i+1}}(\hat{h}^{-1}(\tilde{s}), t) \right\|_{\infty} \right) \\ & \leq \sqrt{n} \sup_{t \in [0, 1]} \sup_{\sqrt{n}|s - \tilde{s}| \leq \frac{\log(n)}{\sqrt{n}}} \left| \hat{U}_{k_{i-1}, k_{i+1}}(h_i^{-1}(s), t) - \hat{U}_{\hat{k}_{i-1}, \hat{k}_{i+1}}(\hat{h}^{-1}(\tilde{s}), t) \right| \end{aligned}$$

on the set where $\sqrt{n}|s_i - \hat{s}_i| \leq \frac{\log(n)}{\sqrt{n}}$ for $i = 1, \dots, m$. This set has probability tending to one which in combination with (6.2) yields the assertion. \square

Lemma 6.3. *Define*

$$\widehat{W}_{i,n}(s, t) := \hat{U}_{k_{i-1}, k_{i+1}}(s, t) - (h_i(s \wedge s_i) - h(s)h_i(s_i))(\mu_i(t) - \mu_{i-1}(t))$$

on the rectangle $[s_{i-1}, s_{i+1}] \times [0, 1]$. Under the assumptions of Theorem 6.4 we have

$$\widehat{W}_n := \begin{pmatrix} \widehat{W}_{1,n}, \widehat{W}_{1,n}^{(1)}, \dots, \widehat{W}_{1,n}^{(R)} \\ \widehat{W}_{2,n}, \widehat{W}_{2,n}^{(1)}, \dots, \widehat{W}_{2,n}^{(R)} \\ \vdots \\ \widehat{W}_{m,n}, \widehat{W}_{m,n}^{(1)}, \dots, \widehat{W}_{m,n}^{(R)} \end{pmatrix} \rightsquigarrow W := \begin{pmatrix} W_1, W_1^{(1)}, \dots, W_1^{(R)} \\ W_2, W_2^{(1)}, \dots, W_2^{(R)} \\ \vdots \\ W_m, W_m^{(1)}, \dots, W_m^{(R)} \end{pmatrix}, \quad (6.3)$$

where $\{W_i^{(1)} | 1 \leq i \leq m\}, \dots, \{W_i^{(R)} | 1 \leq i \leq m\}$ are R independent copies of $\{W_i | 1 \leq i \leq m\}$, which are defined by

$$\{W_i(s, t)\}_{(s,t) \in [s_{i-1}, s_{i+1}] \times [0, 1]} \stackrel{\mathcal{D}}{\sim} \{\mathbb{W}(h_i(s), t)\}_{(s,t) \in [s_{i-1}, s_{i+1}] \times [0, 1]} .$$

Proof. Define

$$\widetilde{W}_n(s, t) = \widehat{W}_n(h_i(s), t) \text{ and } \widetilde{W}(s, t) = W(\hat{h}_i(s), t) . \quad (6.4)$$

Using similar arguments as in the proof of Theorem 6.5 (using the proof of Theorem 4.3 instead of 4.1 from Dette et al. (2020b)) we obtain that each row of \widetilde{W}_n converges weakly to the corresponding row of \widetilde{W} . A straightforward but tedious argument shows that the finite dimensional distributions over both rows and columns \widetilde{W}_n converge weakly to the corresponding finite dimensional distribution of \widetilde{W} . As marginal tightness is equivalent to tightness of the vector we therefore obtain $\widetilde{W}_n \rightsquigarrow \widetilde{W}$. The weak convergence in (6.3) now follows by inverting the operation in (6.4). \square

We now turn to the proof of Theorem 6.4. For this purpose we note that it follows by the same arguments as in Dette et al. (2020b) that $d_H(\hat{\mathcal{E}}_i^{\pm}, \mathcal{E}_i) \xrightarrow{\mathbb{P}} 0$ ($i = 1, \dots, m$), where d_H denotes the Hausdorff distance. The assertion of Theorem 6.4 now follows from Lemma 6.2 and 6.3 in combination with Lemma B.3 in the same reference.

6.3 Proof of Theorem 4.2

For a proof of (i) note that when $\max_{1 \leq i \leq m} \|\mu_i - \mu_{i-1}\|_\infty \leq \Delta$ we have by Theorem 6.1 that

$$\liminf_{n \rightarrow \infty} \mathbb{P}(\{\hat{S}_{\text{rel}} = \emptyset\}) = 1 - \limsup_{n \rightarrow \infty} \mathbb{P}(\hat{T}_n > q_{1-\alpha}^*) \geq 1 - \alpha.$$

For a proof of part (ii) we begin by showing (4.2). For this purpose we note that

$$\begin{aligned} & \{S_{\text{rel}} \subset (\hat{S}_{\text{rel}} + \log(n)/n)\} \\ & \supset \{\hat{T}_{n,i} > q_{1-\alpha}^* \forall i \text{ s.t. } s_i \in S_{\text{rel}}\} \cap \{\hat{m} = m, \max_{1 \leq i \leq m} |\hat{s}_i - s_i| \leq \log(n)/n\} \end{aligned}$$

and recall by the arguments in the proof of Theorem 6.3 that $\hat{T}_{n,i} > q_{1-\alpha}^*$ holds with high probability for any i with $(\|\mu_i - \mu_{i-1}\|_\infty - \Delta) > 0$. By Theorem 4.1 it follows that $\{\hat{m} = m, \max_{1 \leq i \leq m} |\hat{s}_i - s_i| \leq \log(n)/n\}$ holds with high probability which yields the desired assertion.

For equation (4.3) we first note that

$$\{\hat{S}_{\text{rel}} \subset (S_{\text{rel}} + \log(n)/n)\} \supset \{\hat{T}_{n,i} \leq q_{1-\alpha}^*, i \text{ s.t. } s_i \notin S_{\text{rel}}\} \cap \{S_r \subset (\hat{S}_{\text{rel}} + \log(n)/n)\}$$

and that

$$\mathbb{P}(\max_{i \notin S_{\text{rel}}} \hat{T}_{n,i} > q_{1-\alpha}^*) \geq 1 - \alpha \tag{6.5}$$

by Theorem 6.1. For equation (4.4) note that the inequality (6.5) can be improved to $1 - o(1)$ whenever

$$\max_{1 \leq i \leq m, s_i \notin S_{\text{rel}}} \|\mu_i - \mu_{i-1}\|_\infty < \Delta$$

observing the inequality

$$\hat{T}_n \leq \hat{D}_n + \sqrt{n} \left(\max_{1 \leq i \leq m, s_i \notin S_{\text{rel}}} \|\mu_i - \mu_{i-1}\|_\infty - \Delta \right)$$

and that \hat{D}_n is tight.